



HIGH PRECISION AT HADRON MACHINES

Roger J. Hernández Pinto
Facultad de Ciencias Físico-Matemáticas
Universidad Autónoma de Sinaloa

based on: arXiv:1410.6027, arXiv:1506.04617, arXiv:1604.06699.

Seminario del Cuerpo Académico de Partículas, Campos y Relatividad General
FCFM - BUAP
May 26th, 2016

OUTLINE

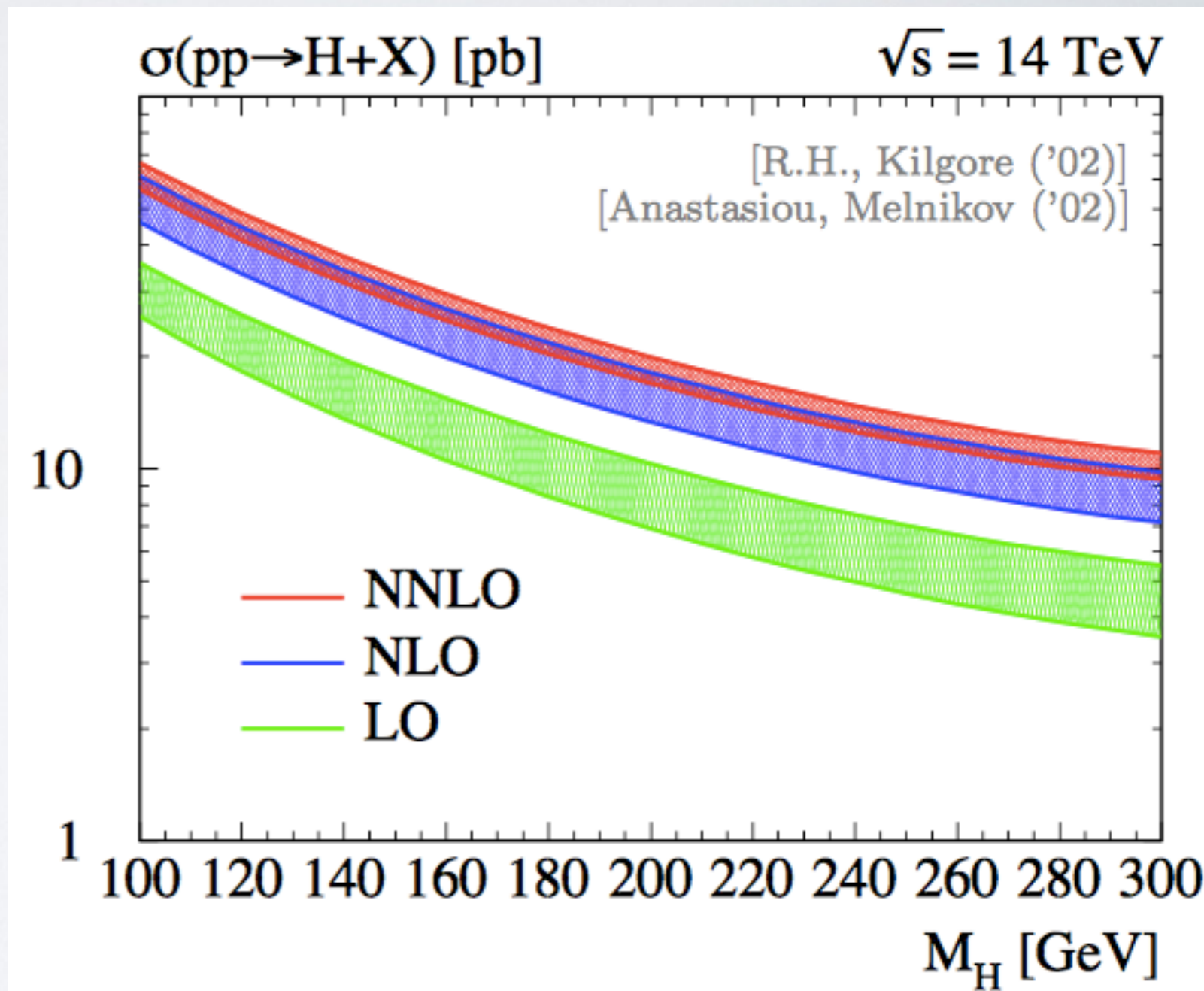
- Introduction to high accuracy at the LHC
- High precision at fixed order
 - Perturbative calculations
 - Non-perturbative determinations
- Conclusions

— *Physics at the LHC* —

- LHC experiments are delivering more and more data to the HEP community.
- More data sets improve the accuracy of all observables.
- And, when the physics is hidden in small effects, accuracy is crucial to claim discovery.
- The new 750 GeV resonance !

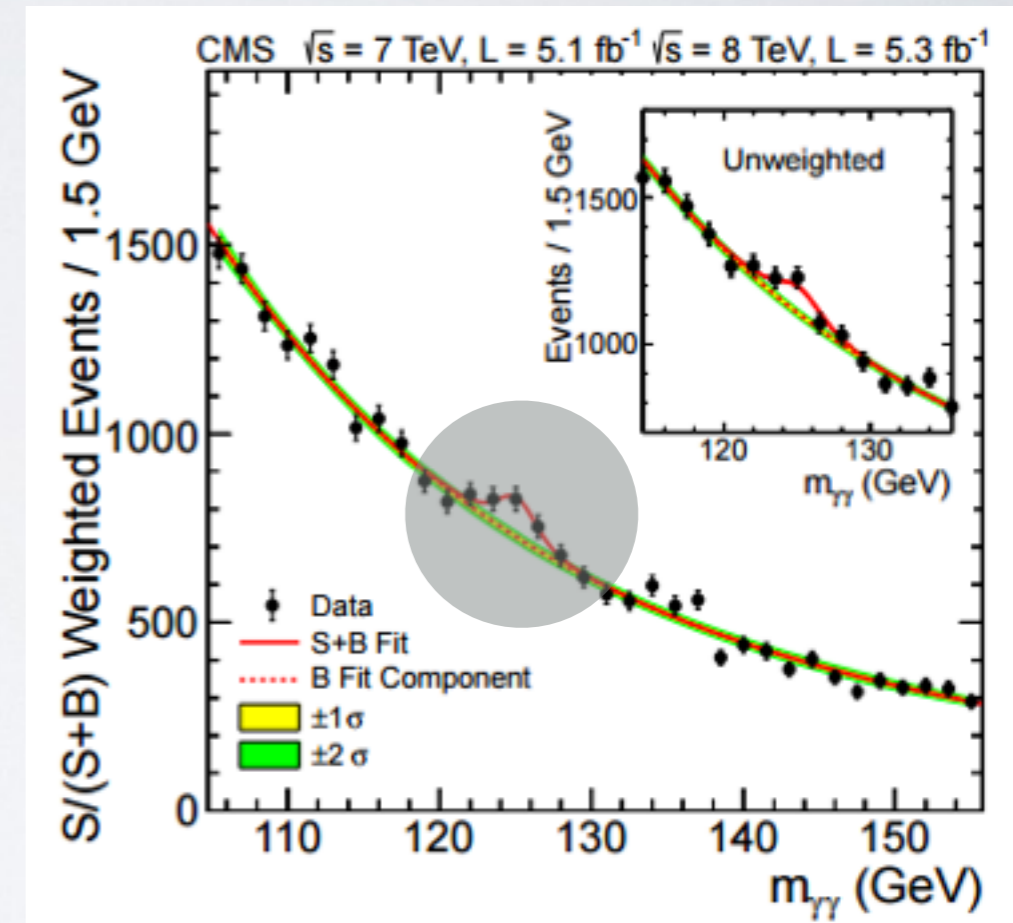
— *High Precision* —

- LO do not even provides the order of magnitude of the cross section.
- Virtual corrections could have an enormous impact for the LHC physics program.
- High precision requires the computation of new Feynman diagrams.



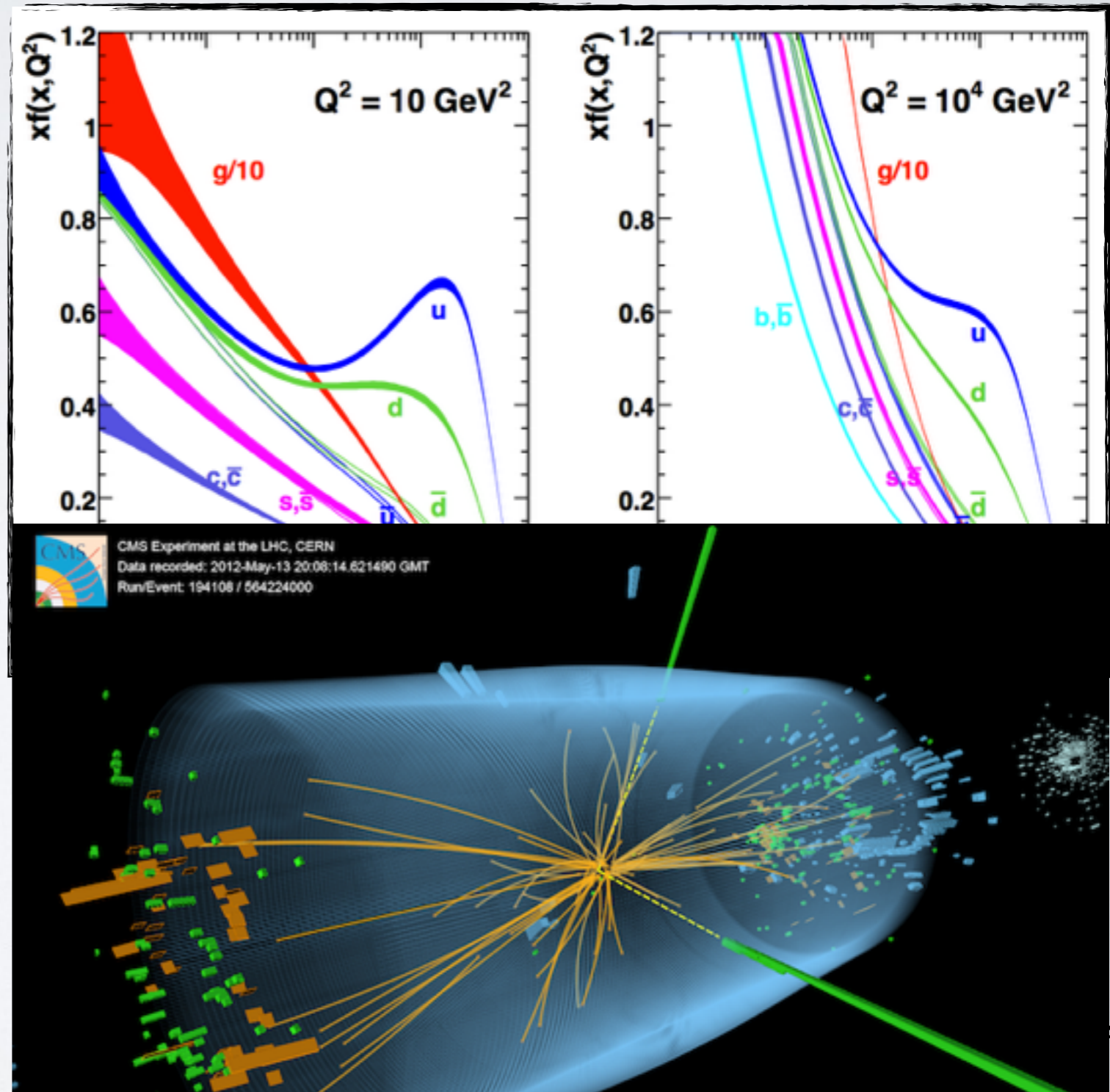
— *Higgs discovery* —

- In 2012 at CERN, ATLAS and CMS announced a 5sigma evidence of a resonance around 125 GeV.
- The claim was that the bosonic particle is the SM-Higgs.
- Determination of properties of new particles and New Physics requires precision measurements.



— *Hadron machines* —

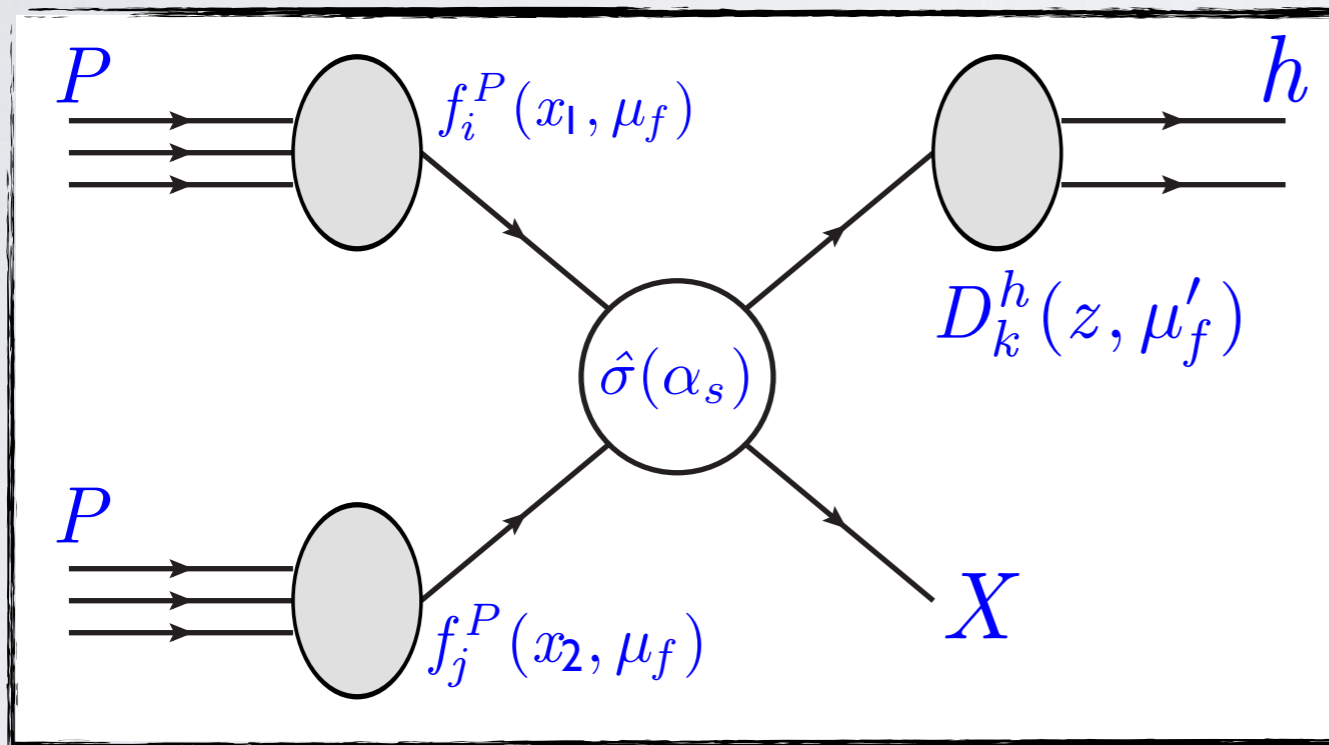
- Hadron machines are dominated by gluon densities (QCD).
- Fundamental particles are only detected indirectly.



- New Physics has to be disentangled from Standard Model physics. High precision in SM calculations.
- Hadron machines are dominated by QCD effects. Exact solutions of QCD are not known, then pQCD helps to compute scattering amplitudes.
- However, high accuracy on LHC observables requires higher orders in pQCD.
- Besides, high level of accuracy is reached when the perturbative and non-perturbative pieces are under control at fixed order in pQCD.

— Setup at hadron machines —

- How to translate theoretical predictions to experimental measurements ?



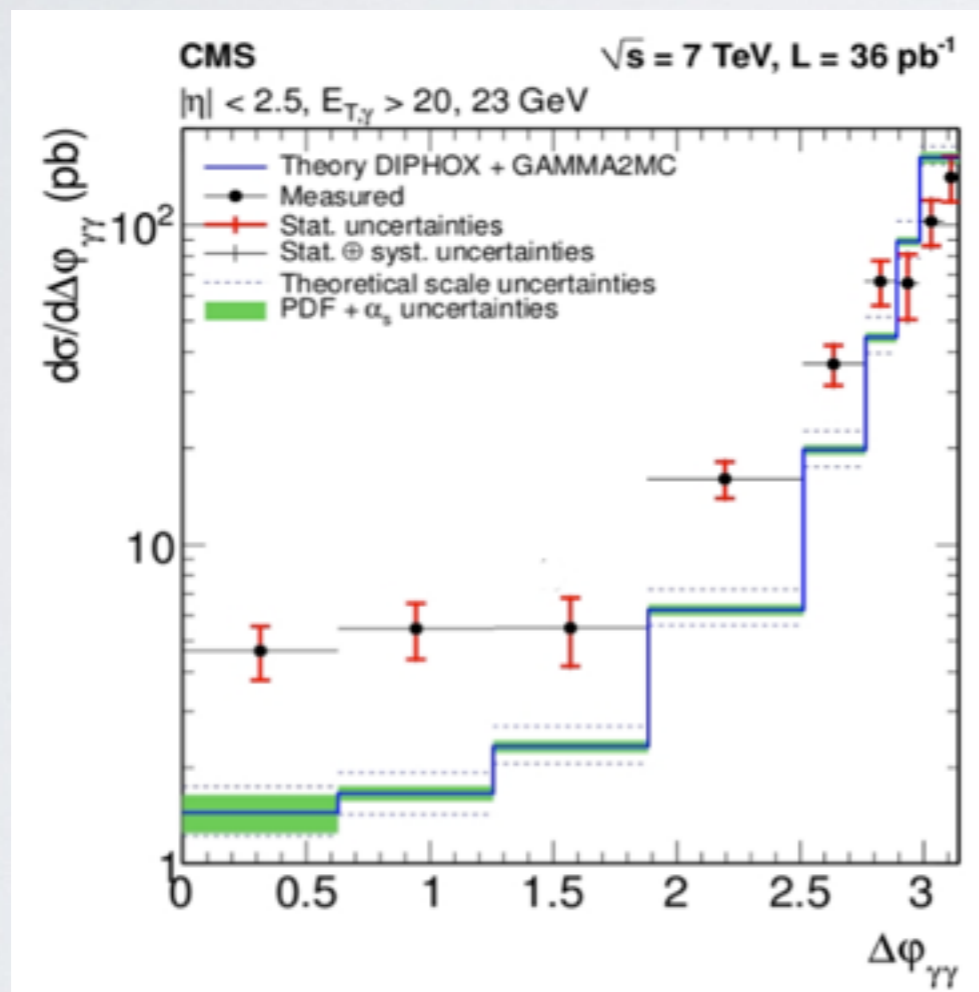
Perturbative

Non Perturbative

$$\frac{d\sigma(pp \rightarrow hX)}{dp_T d\eta} = \sum_{i,j,k} \int dx_1 dx_2 dz \left(f_i^P \otimes f_j^P \otimes D_k^h \otimes \frac{d\hat{\sigma}(ij \rightarrow kX')}{dp_T d\eta} \right)$$

— *Theory meets experiment* —

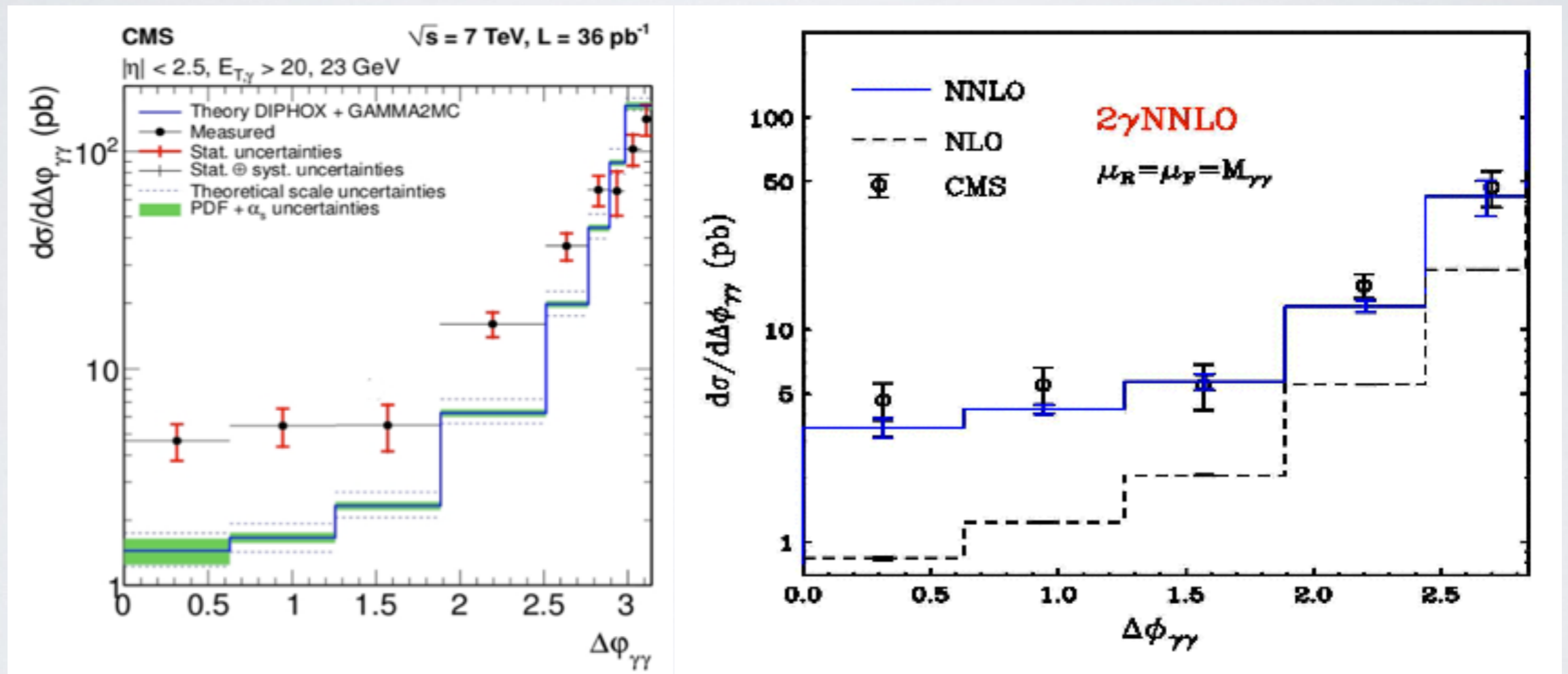
- Precision measurements use accurate theoretical predictions.



- Experimental results needs Monte Carlo simulations in order to compare with nature.

— *Theory meets experiment* —

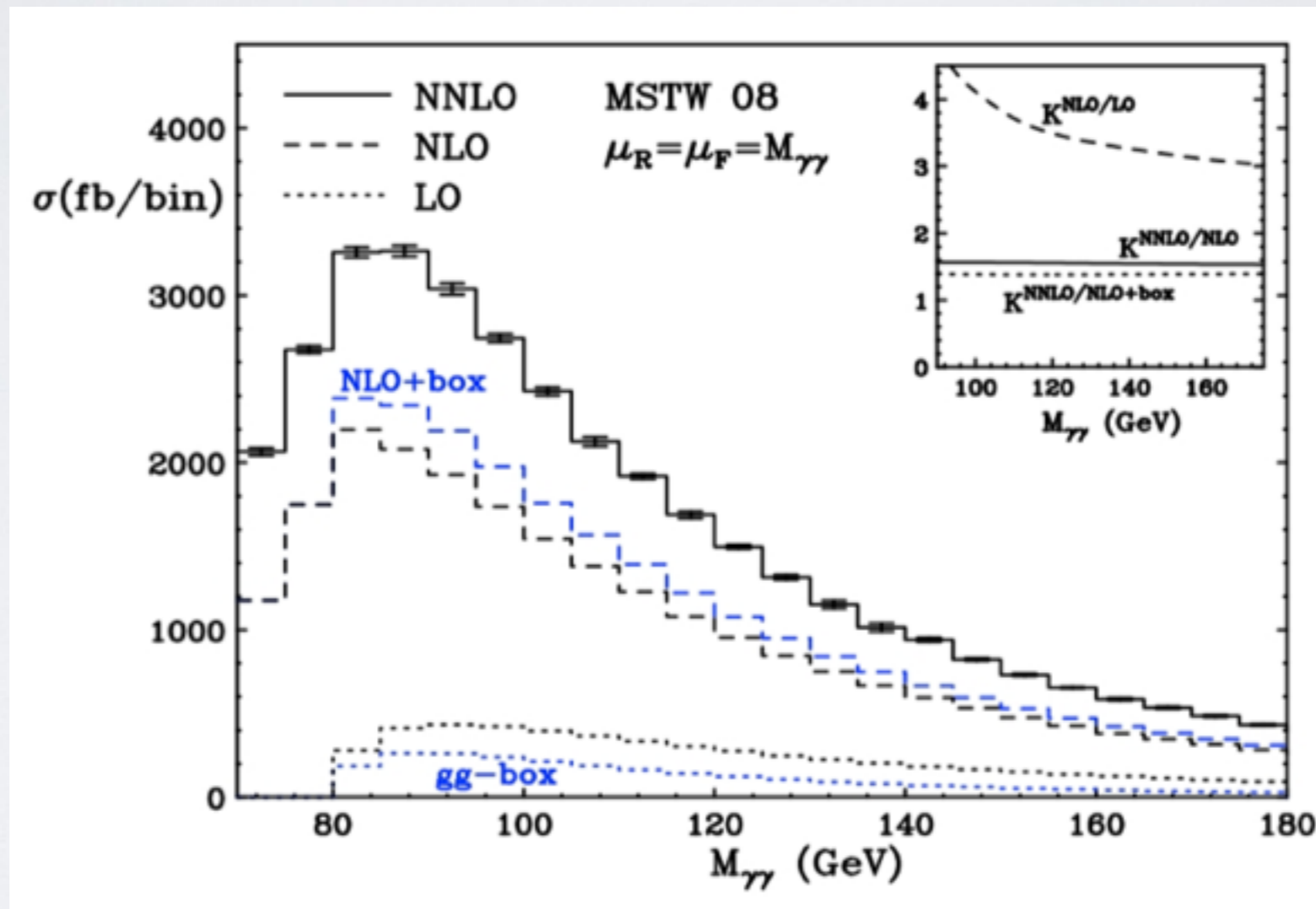
- Precision measurements use accurate theoretical predictions.



- Experimental results needs Monte Carlo simulations in order to compare with nature.

— *and for the next run(s)* —

- Moreover, future observables need accurate Monte Carlo simulations.



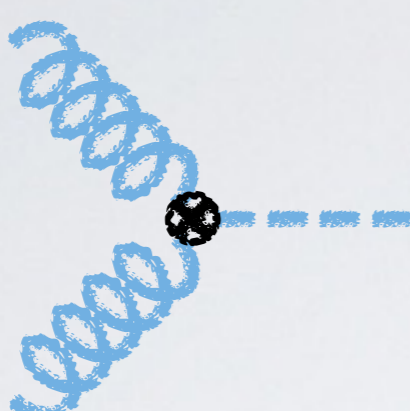
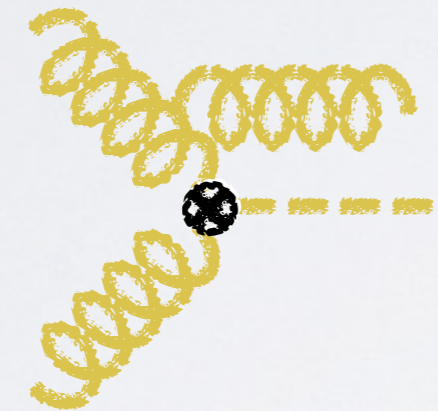
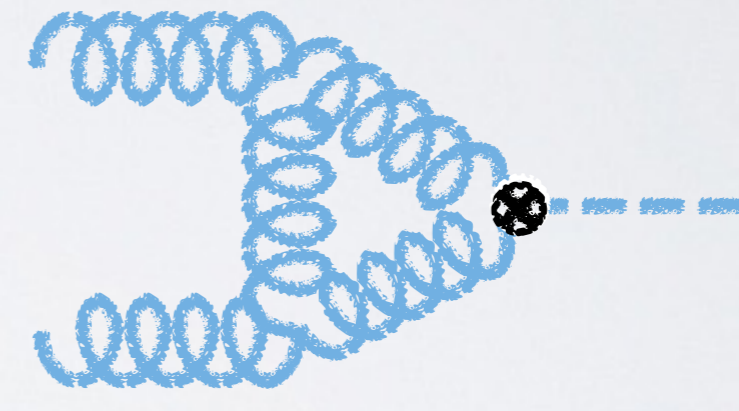
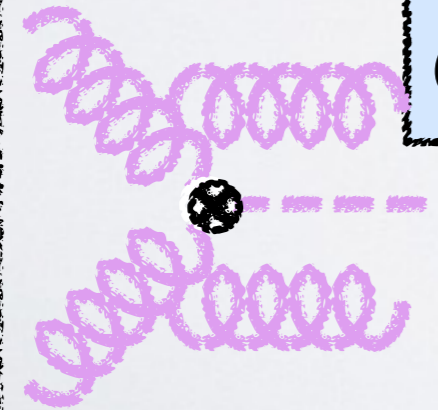

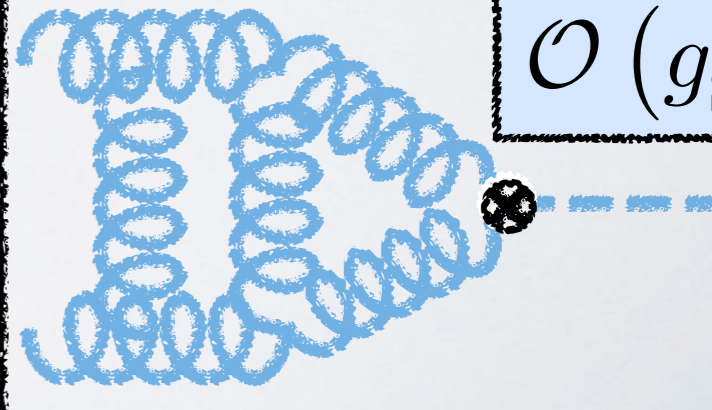
- Relevant contributions will only be explained when NNLO Monte Carlo simulations are implemented.

PERTURBATIVE TOOLS

— *Dimensional regularisation (DREG)* —

- DREG promotes 4-dimensional integrals to d -dimensional integrals ($d = 4 - 2\epsilon$).
- Divergences appear like poles in the dimensional parameter ϵ .
- Loop integrals generate UV and IR poles.
- UV (High energy region) poles are cured with proper counterterms.
- IR (Low energy region) poles are cured by adding real emission processes.

@ amplitude level

<p>LO</p>	 <p>$\mathcal{O}(g_S^2)$</p>	<p>Phase space</p> <p>2 → 1 2 → 2 2 → 3</p>	
<p>NLO</p>	 <p>$\mathcal{O}(g_S^3)$</p> <p>real correction</p>	 <p>$\mathcal{O}(g_S^4)$</p> <p>virtual correction</p>	
<p>NNLO</p>	 <p>$\mathcal{O}(g_S^4)$</p> <p>RR-correction</p>	 <p>$\mathcal{O}(g_S^5)$</p> <p>VR-correction</p>	 <p>$\mathcal{O}(g_S^6)$</p> <p>VV-correction</p>

- The total cross section is computed as,

$$\sigma = \sigma^{(LO)} + \alpha_S(\mu)\sigma^{(NLO)} + \alpha_S^2(\mu)\sigma^{(NNLO)} + \dots$$

- where

$$\sigma^{(NLO)} = \int_{\Omega} d\sigma^V + \int_{\Omega+1} d\sigma^R$$

$$\sigma^{(NNLO)} = \int_{\Omega} d\sigma^{VV} + \int_{\Omega+1} d\sigma^{RV} + \int_{\Omega+2} d\sigma^{RR}$$

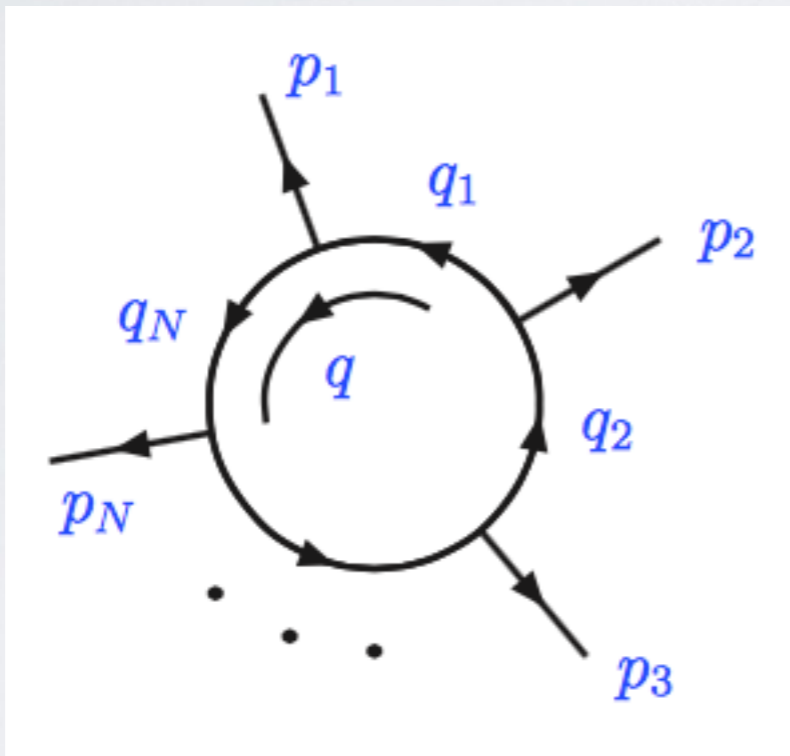
- and divergences are everywhere.

— *Theoretical issues* —

- Integrands are usually lengthy.
- The number of Feynman diagrams increase enormously when high accuracy is required.
- Monte Carlo simulations first compute the poles and shows the exact cancellation at integral-level. Then, it computes the number of integrals separately (2 at NLO, 3 at NNLO, etc.).
- New Physics searches have to be done at the highest possible accuracy.
- New methods for higher order calculations are extremely important.

— *Loop-Tree duality* —

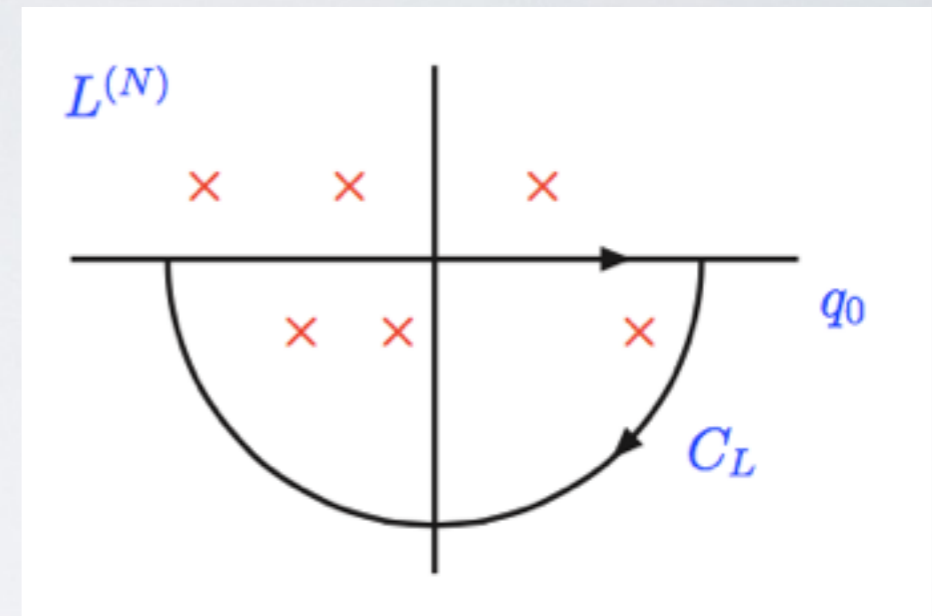
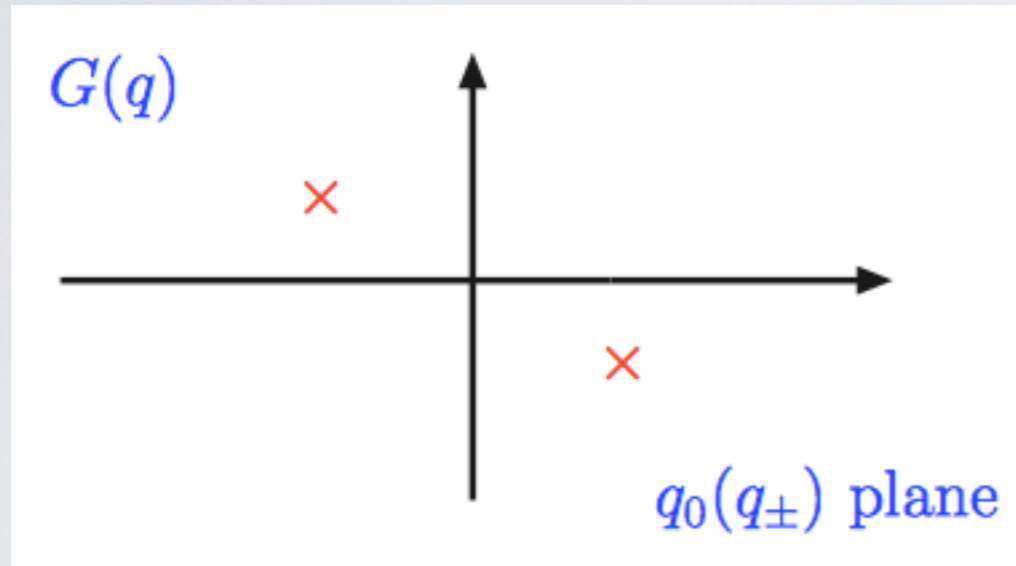
- Massive one-loop scalar integrals are,



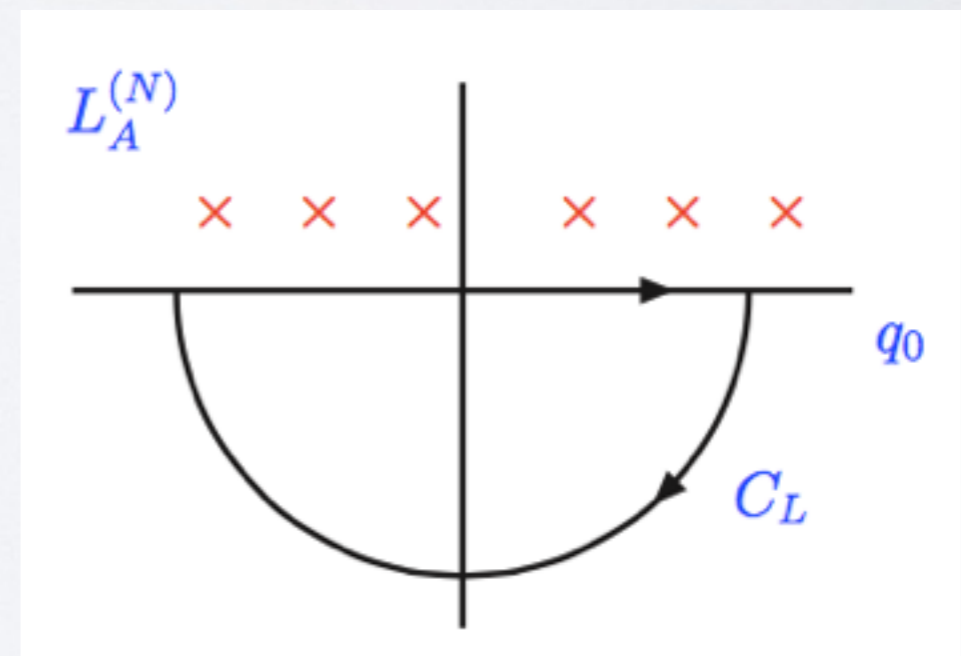
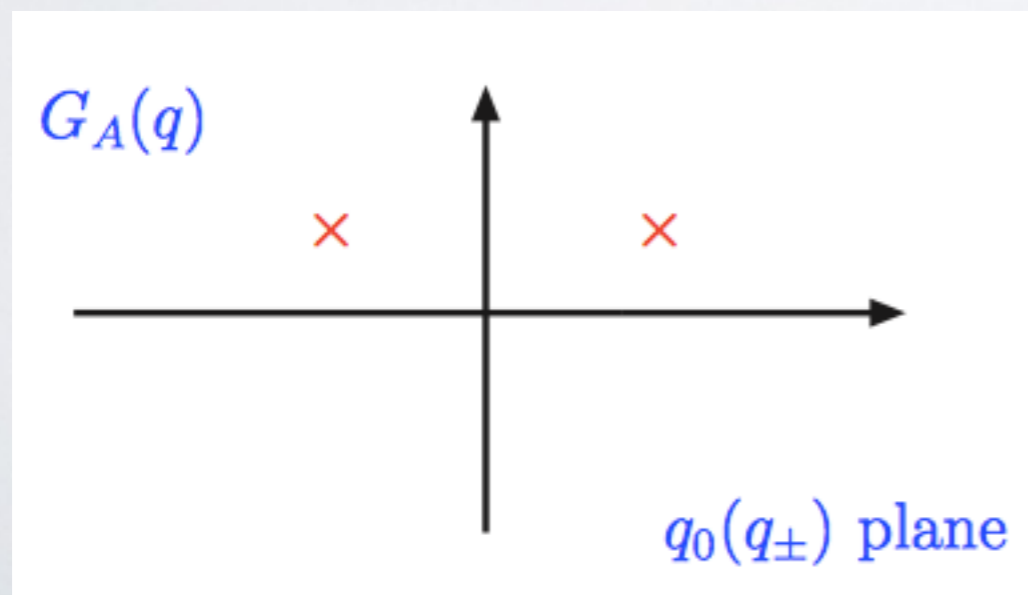
$$= -i \int \frac{d^d q}{(2\pi)^d} \prod_{i=1}^N \frac{1}{q_i^2 - m_i^2 + i0}$$

- where the $+i0$ prescription establishes that particles are going forward in time.

- The solution of the integrals are known by the Cauchy residues theorem.



- However, by using advanced propagators,



- LTD at one loop establishes then

$$L^{(1)}(p_1, \dots, p_N) = - \sum \int_{\ell_1} \tilde{\delta}(q_i) \prod_{\substack{j=1 \\ j \neq i}}^N G_D(q_i; q_j)$$

- where Feynman propagators are transformed to dual propagators.

$$G_D(q_i; q_j) = \frac{1}{q_j^2 - m_j^2 - i0\eta \cdot (q_j - q_i)}$$

- $\tilde{\delta}(q_i) = 2\pi i \theta(q_{i,0}) \delta(q_i^2 - m_i^2)$ and sets internal lines on-shell and in the positive energy mode.
- LTD modify the $+i0$ prescription, instead of having multiple cuts like in the Feynman Tree Theorem.
- η^μ is a future-like vector, for simplicity we take $\eta^\mu = (1, \mathbf{0})$. In fact, the only relevance is the sign in the prescription.

— *Numerical implementation* —

- Faster computations are needed for the Montecarlo simulations for the LHC observables.
- Using LTD the standard methods become time consuming
- (S. Buchta, et al., arXiv:1510.00187)

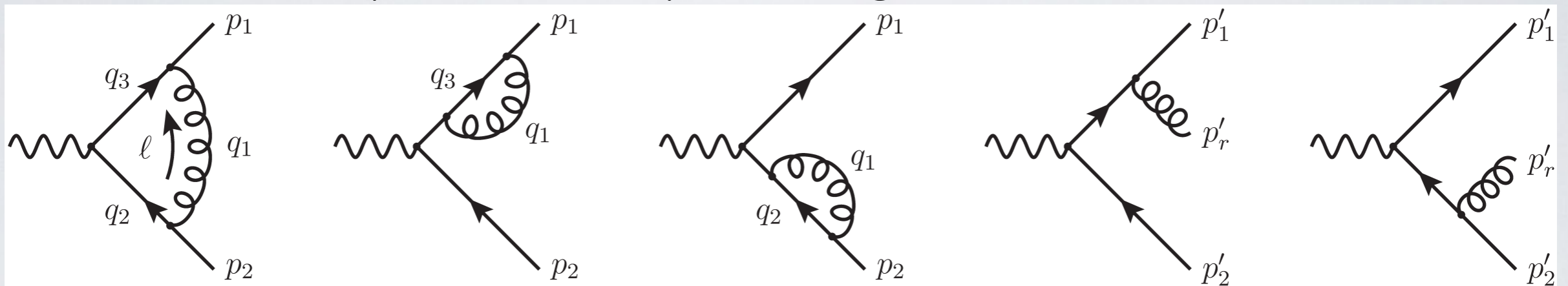
	Rank	Tensor Pentagon	Real Part	Imaginary Part	Time [s]
P16	2	LoopTools	-1.86472×10^{-8}		
		SecDec	$-1.86471(2) \times 10^{-8}$		45
		LTD	$-1.86462(26) \times 10^{-8}$		1
P17	3	LoopTools	1.74828×10^{-3}		
		SecDec	$1.74828(17) \times 10^{-3}$		550
		LTD	$1.74808(283) \times 10^{-3}$		1
P18	2	LoopTools	-1.68298×10^{-6}	$+i 1.98303 \times 10^{-6}$	
		SecDec	$-1.68307(56) \times 10^{-6}$	$+i 1.98279(90) \times 10^{-6}$	66
		LTD	$-1.68298(74) \times 10^{-6}$	$+i 1.98299(74) \times 10^{-6}$	36
P19	3	LoopTools	-8.34718×10^{-2}	$+i 1.10217 \times 10^{-2}$	
		SecDec	$-8.33284(829) \times 10^{-2}$	$+i 1.10232(107) \times 10^{-2}$	1501
		LTD	$-8.34829(757) \times 10^{-2}$	$+i 1.10119(757) \times 10^{-2}$	38

	Rank	Tensor Hexagon	Real Part	Imaginary Part	Time[s]
P20	1	SecDec	$-1.21585(12) \times 10^{-15}$		36
		LTD	$-1.21552(354) \times 10^{-15}$		6
P21	3	SecDec	$4.46117(37) \times 10^{-9}$		5498
		LTD	$4.461369(3) \times 10^{-9}$		11
P22	1	SecDec	$1.01359(23) \times 10^{-15}$	$+i 2.68657(26) \times 10^{-15}$	33
		LTD	$1.01345(130) \times 10^{-15}$	$+i 2.68633(130) \times 10^{-15}$	72
P23	2	SecDec	$2.45315(24) \times 10^{-12}$	$-i 2.06087(20) \times 10^{-12}$	337
		LTD	$2.45273(727) \times 10^{-12}$	$-i 2.06202(727) \times 10^{-12}$	75
P24	3	SecDec	$-2.07531(19) \times 10^{-6}$	$+i 6.97158(56) \times 10^{-7}$	14280
		LTD	$-2.07526(8) \times 10^{-6}$	$+i 6.97192(8) \times 10^{-7}$	85

- This results shows have been implemented for several data points for tensor pentagons and hexagons.
- Integrals considering massive internal lines were computed numerically.
- The results using LTD are, in some cases, four order of magnitudes faster than SecDec.
- What about in a physical process ?

$\gamma^* \rightarrow q\bar{q}$ at NLO in QCD

- In this well known process, the Feynman diagrams are



- where the process add more structure to the integrals. In general, virtual and real corrections have numerators.
- In this case, for the virtual correction is given by,

$$\langle \mathcal{M}_{q\bar{q}}^{(0)} | \mathcal{M}_{q\bar{q}}^{(1)} \rangle = g_S^2 C_F |\mathcal{M}_{q\bar{q}}^{(0)}|^2 \frac{4}{s_{12}} \int_{\ell} \left(\prod_{i=1}^3 G_F(q_i) \right) \times \epsilon \left[(2 + \epsilon)(q_2 \cdot p_1)(q_3 \cdot p_2) - \epsilon \left((q_2 \cdot p_2)(q_3 \cdot p_1) + \frac{s_{12}}{2}(q_2 \cdot q_3) \right) \right]$$

- and for the real correction is,

$$\sigma_R^{(1)} = \sigma^{(0)} \frac{(4\pi)^{\epsilon-2}}{\Gamma(1-\epsilon)} g_S^2 C_F \left(\frac{s_{12}}{\mu^2} \right)^{-\epsilon} \int_0^1 dy'_{1r} \int_0^{1-y'_{1r}} dy'_{2r} (y'_{1r} y'_{2r} y'_{12})^{-\epsilon} \\ \times \left[4 \left(\frac{y'_{12}}{y'_{1r} y'_{2r}} - \epsilon \right) + 2(1-\epsilon) \left(\frac{y'_{2r}}{y'_{1r}} + \frac{y'_{1r}}{y'_{2r}} \right) \right]$$

- Using DREG, the result is,

$$\sigma_V^{(1)} = \sigma^{(0)} c_\Gamma g_S^2 C_F \left(\frac{s_{12}}{\mu^2} \right)^{-\epsilon} \left[-\frac{4}{\epsilon^2} - \frac{6}{\epsilon} - 16 + 2\pi^2 + \mathcal{O}(\epsilon) \right]$$

$$\sigma_R^{(1)} = \sigma^{(0)} c_\Gamma g_S^2 C_F \left(\frac{s_{12}}{\mu^2} \right)^{-\epsilon} \left[\frac{4}{\epsilon^2} + \frac{6}{\epsilon} + 19 - 2\pi^2 + \mathcal{O}(\epsilon) \right]$$

- Then,

$$\sigma = \sigma^{(0)} \left(1 + 3C_F \frac{\alpha_S}{4\pi} + \mathcal{O}(\alpha_S^2) \right)$$

Remarks:

- IR behaviour is quite similar to the scalar case, therefore the same mapping is performed.
- There is no need of tensor reduction, no need of Gram determinants.
- Two point function of massless particles are usually ignored because is scaleless.
- In fact, this integral is zero because IR and UV poles cancels.
- In the LTD, there is an identification of IR and UV regions, therefore it has to be consider at the integrand level.

- Following the procedure described, it is possible to find 4-dimensional representations for the cross sections, resulting:

$$\tilde{\sigma}_1^{(1)} = \sigma^{(0)} \frac{\alpha_S}{4\pi} C_F \int_0^1 d\xi_{1,0} \int_0^{1/2} dv_1 4 \mathcal{R}_1(\xi_{1,0}, v_1) \left[2 (\xi_{1,0} - (1 - v_1)^{-1}) - \frac{\xi_{1,0}(1 - \xi_{1,0})}{(1 - (1 - v_1) \xi_{1,0})^2} \right],$$

$$\begin{aligned} \tilde{\sigma}_2^{(1)} = \sigma^{(0)} \frac{\alpha_S}{4\pi} C_F \int_0^1 d\xi_{2,0} \int_0^1 dv_2 2 \mathcal{R}_2(\xi_{2,0}, v_2) (1 - v_2)^{-1} & \left[\frac{2 v_2 \xi_{2,0} (\xi_{2,0}(1 - v_2) - 1)}{1 - \xi_{2,0}} \right. \\ & \left. - 1 + v_2 \xi_{2,0} + \frac{1}{1 - v_2 \xi_{2,0}} \left(\frac{(1 - \xi_{2,0})^2}{(1 - v_2 \xi_{2,0})^2} + \xi_{2,0}^2 \right) \right], \end{aligned}$$

$$\begin{aligned} \bar{\sigma}_V^{(1)} = \sigma^{(0)} \frac{\alpha_S}{4\pi} C_F \int_0^\infty d\xi \int_0^1 dv & \left\{ -2 (1 - \mathcal{R}_1(\xi, v)) v^{-1} (1 - v)^{-1} \frac{\xi^2 (1 - 2v)^2 + 1}{\sqrt{(1 + \xi)^2 - 4v\xi}} \right. \\ & + 2 (1 - \mathcal{R}_2(\xi, v)) (1 - v)^{-1} \left[2 v \xi (\xi(1 - v) - 1) \left(\frac{1}{1 - \xi + i0} + v\pi\delta(1 - \xi) \right) - 1 + v \xi \right] \\ & + 2 v^{-1} \left(\frac{\xi(1 - v)(\xi(1 - 2v) - 1)}{1 + \xi} + 1 \right) - \frac{(1 - 2v) \xi^3 (12 - 7m_{UV}^2 - 4\xi^2)}{(\xi^2 + m_{UV}^2)^{5/2}} \\ & \left. - \frac{2 \xi^2 (m_{UV}^2 + 4\xi^2(1 - 6v(1 - v)))}{(\xi^2 + m_{UV}^2)^{5/2}} \right\}, \end{aligned}$$

- Then, these integrals in 4D are solvable analytically, resulting:

$$\tilde{\sigma}_1^{(1)} = \sigma^{(0)} \frac{\alpha_S}{4\pi} C_F (19 - 32 \log(2)),$$

$$\tilde{\sigma}_2^{(1)} = \sigma^{(0)} \frac{\alpha_S}{4\pi} C_F \left(-\frac{11}{2} + 8 \log(2) - \frac{\pi^2}{3} \right),$$

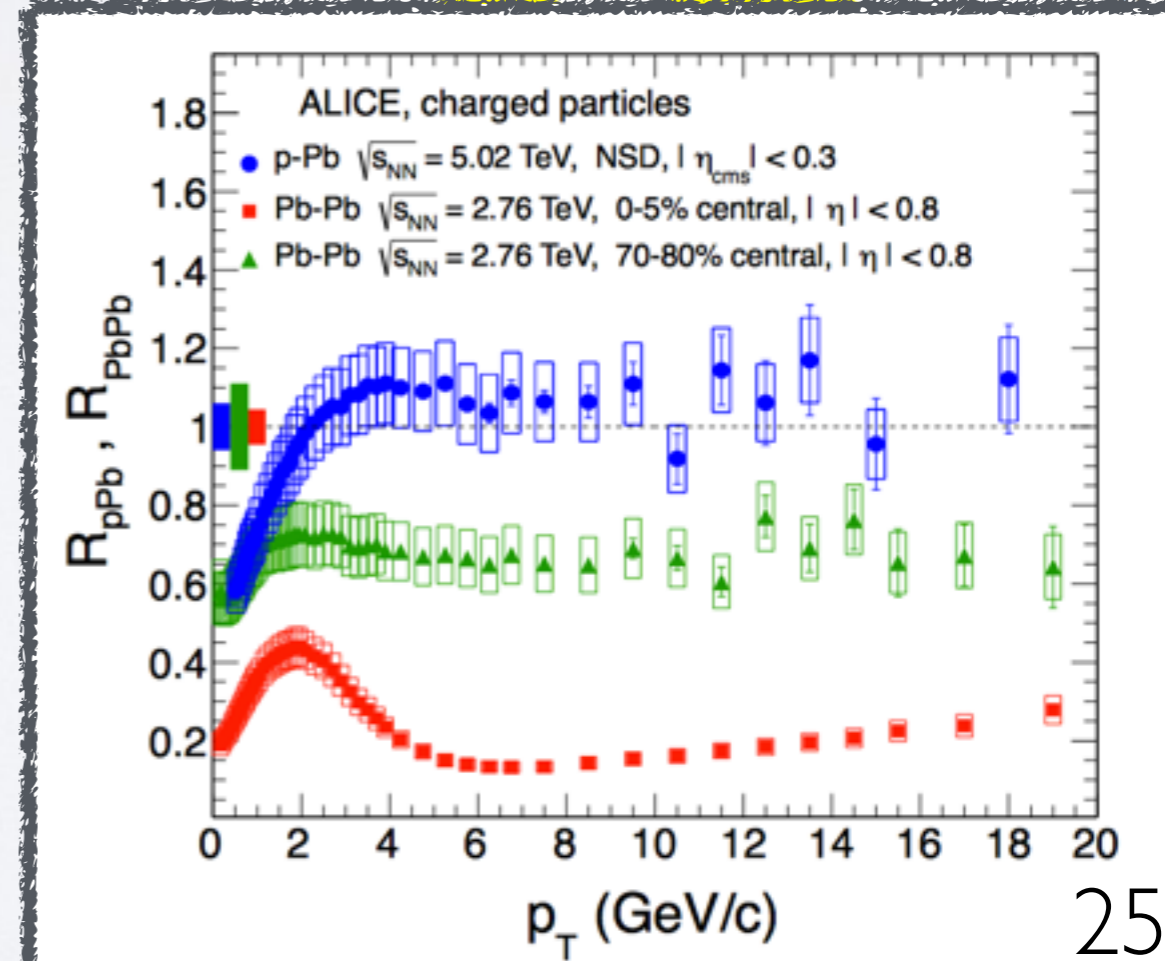
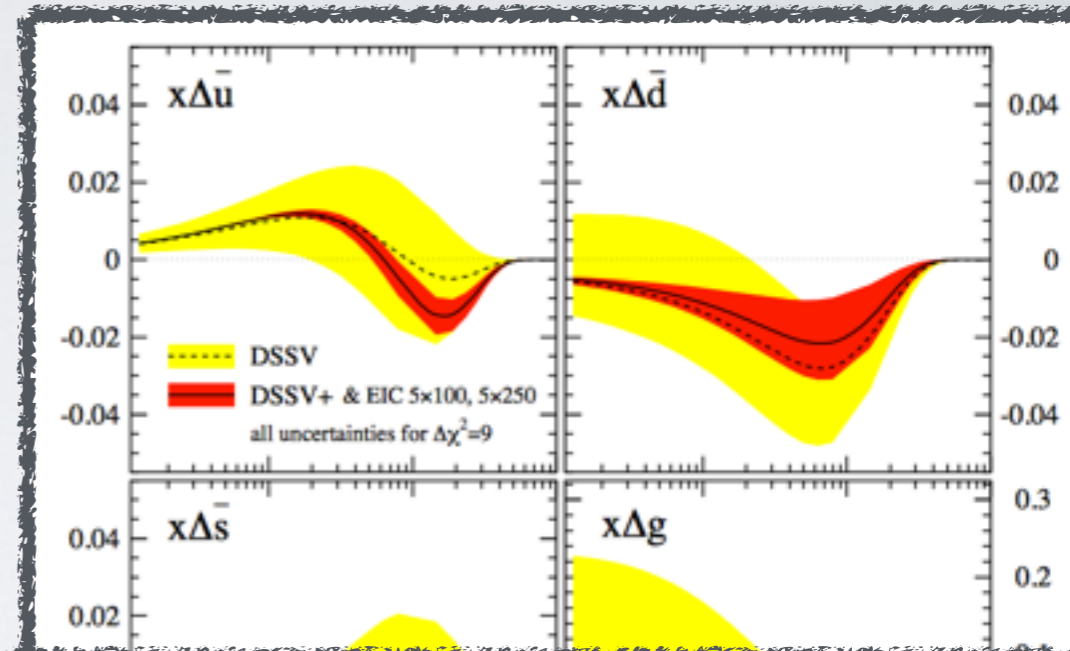
$$\bar{\sigma}_V^{(1)} = \sigma^{(0)} \frac{\alpha_S}{4\pi} C_F \left(-\frac{21}{2} + 24 \log(2) + \frac{\pi^2}{3} \right).$$

- Thus: $\tilde{\sigma}_1^{(1)} + \tilde{\sigma}_2^{(1)} + \bar{\sigma}_V^{(1)} = \sigma^{(0)} 3C_F \frac{\alpha_S}{4\pi}$
- Computation of multi-legs and NNLO corrections are doable within the LTD.

NON PERTURBATIVE DISTRIBUTIONS

— Motivation of FFs —

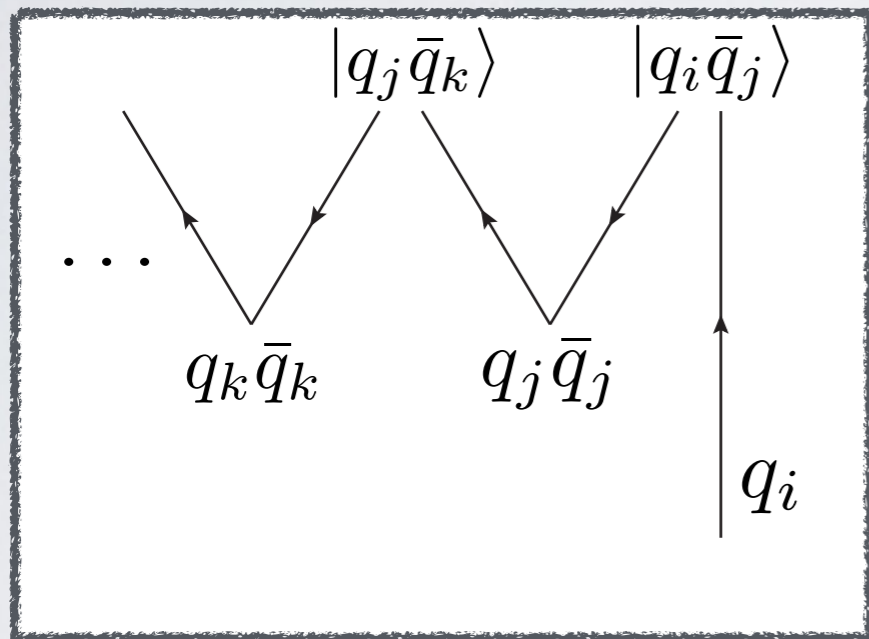
- Input for helicities PDFs and transverse momentum PDFs.
- Necessary for a complete understanding of hadron production in presence of nuclear medium.
- Heavy Ion programs: RHIC and LHC.



— Theory & Uncertainties —

Basic idea of hadronization: Cascade fragmentation

Rank 2 1



rank = 1 : “valence”, e.g.

$$u \rightarrow \pi^+$$

rank > 2 : “sea”, e.g.

$$u \rightarrow \pi^-$$

- Theory framework: “independent fragmentation”.
- QCD approach based on factorization.
- e^+e^- : first data used for extracting FFs with LEP data (BKK '95 and KRE '00).

The fitters

Name	Ref.	Species	Error	z_{\min}	Q^2 (GeV ²)
AKK	[4]	$\pi^\pm, K^\pm, K_s^0, p, p, \Lambda, \Lambda$	no	0.1	$2 - 4 \cdot 10^4$
AKK08	[5]	$\pi^\pm, K^\pm, K_s^0, p, p, \Lambda, \Lambda$	yes	0.05	$2 - 4 \cdot 10^4$
BKK	[6]	$\pi^+ + \pi^-, \pi^0, K^+ + K^-, K^0 + K^0, h^+ + h^-$	no	0.05	$2 - 200$
BFG	[7]	γ	no	10^{-3}	$2 - 1.2 \cdot 10^4$
BFGW	[8]	h^\pm	yes ¹	10^{-3}	$2 - 1.2 \cdot 10^4$
CGRW	[9]	π^0	no	10^{-3}	$2 - 1.2 \cdot 10^4$
DSS	[10,11]	$\pi^\pm, K^\pm, p, p, h^\pm$	yes ²	0.05-0.1	$1 - 10^5$
DSV	[12]	polarized and unpolarized Λ	no	0.05	$1 - 10^4$
GRV	[13]	γ	no	0.05	≥ 1
HKNS	[14]	$\pi^\pm, \pi^0, K^\pm, K^0 + K^0, n, p + p$	yes	0.01 - 1	$1 - 10^8$
KKP	[15]	$\pi^+ + \pi^-, \pi^0, K^+ + K^-, K^0 + K^0, p + p, n + n, h^+ + h^-$	no	0.1	$1 - 10^4$
Kretzer	[16]	$\pi^\pm, K^\pm, h^+ + h^-$	no	0.01	$0.8 - 10^6$

- AKK08: e⁺e⁻ and pp data / Isospin symmetry for pions.
- HKNS: e⁺e⁻ data only / Hessian method for uncertainties.

DSS results

- DSS fit arrived to a data-driven separation of individual parton-to-pion fragmentations.
- Large charge symmetry violation between u- and d-quarks FFs ($\sim 10\%$).
- Gluon FFs was constrained for the first time with BNL-RHIC data.
- Lagrange multiplier technique was used for estimating uncertainties.

FFs in data: e^+e^- SIA

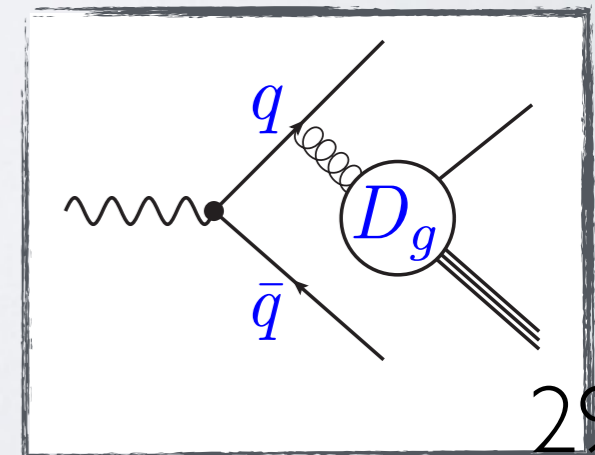
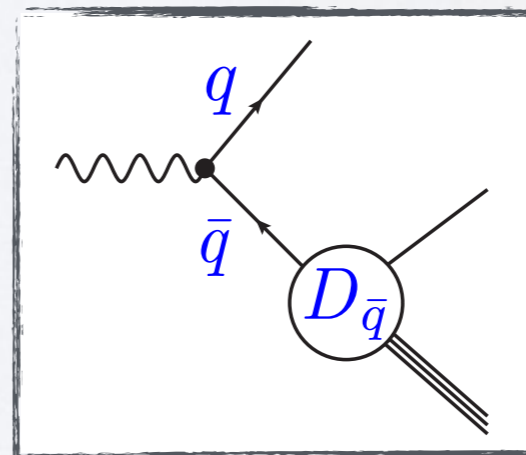
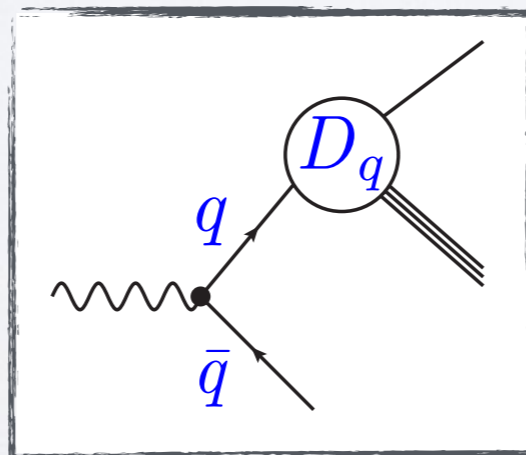
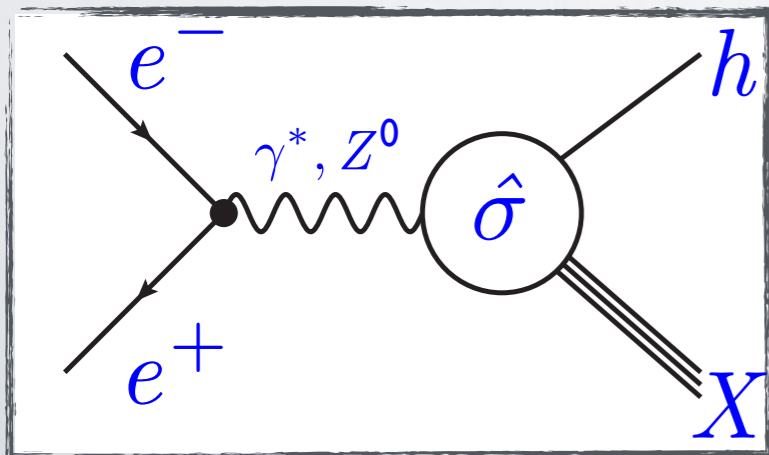
- The distribution is given terms of the structure functions,

$$\frac{1}{\sigma_{tot}} \frac{d\sigma^h}{dz} = \frac{\sigma^0}{\sum_q \hat{e}_q^2} [2F_1^h(z, Q^2) + F_L^h(z, Q^2)]$$

@NLO

$$2F_1^h(z, Q^2) = \sum_q \hat{e}_q^2 \left\{ [D_q^h + D_{\bar{q}}^h](z, Q^2) + \frac{\alpha_s(Q^2)}{2\pi} [C_q^1 \otimes [D_q^h + D_{\bar{q}}^h] + C_g^1 \otimes D_g^h](z, Q^2) \right\}$$

- Not possible to separate charge and flavour only with SIA.
- Only have information of the singlet.



FFs in data: SIDIS

- Distributions for SIDIS are given by,

$$\frac{d\sigma^h}{dx dy dz^h} = \frac{2\pi\alpha_s(Q^2)}{Q^2} \left[\frac{1 + (1-y)^2}{y} 2F_1^h + \frac{2(1-y)}{y} F_L^h \right] (x, z_h, Q^2)$$

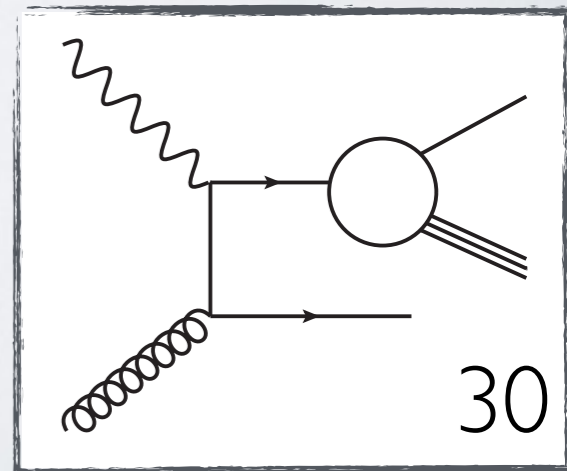
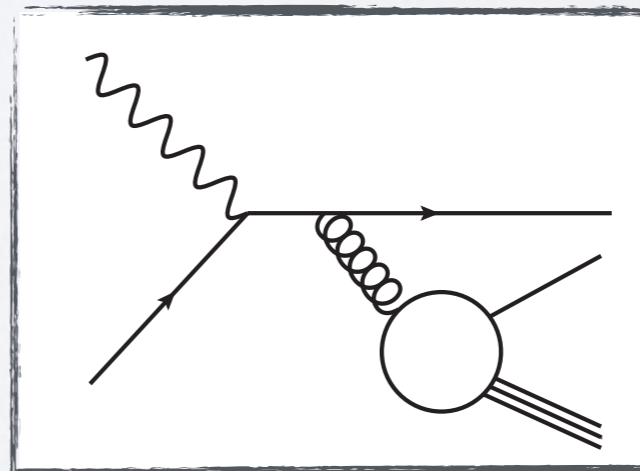
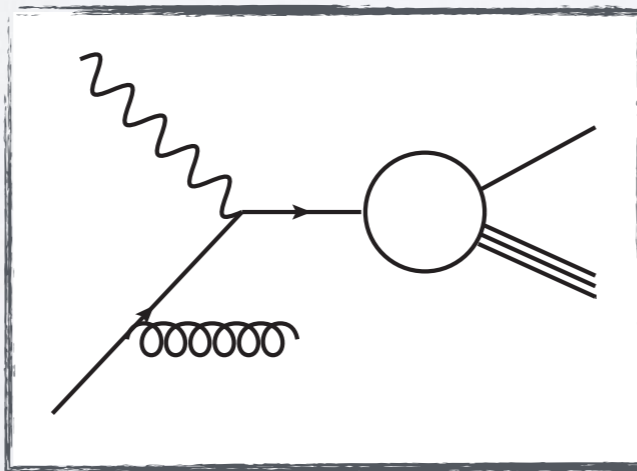
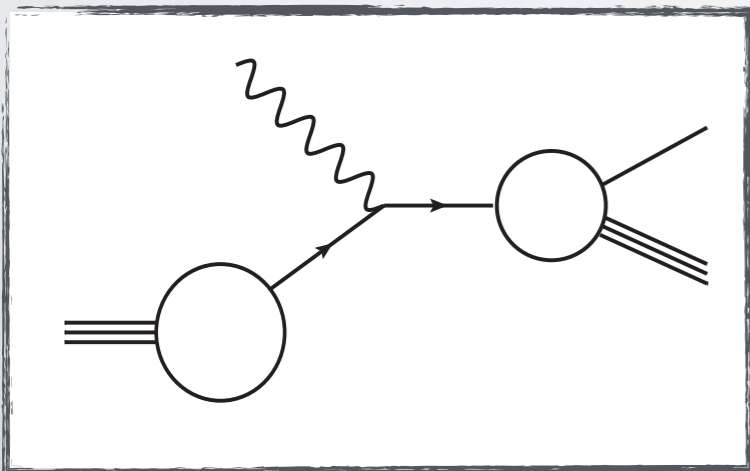
@LO:

$$2F_1^h(x, z_h, Q^2) = \sum_{q, \bar{q}} \hat{e}_q^2 \cdot q(x, Q^2) D_q^h(z_h, Q^2)$$

@NLO, all coefficients are known:

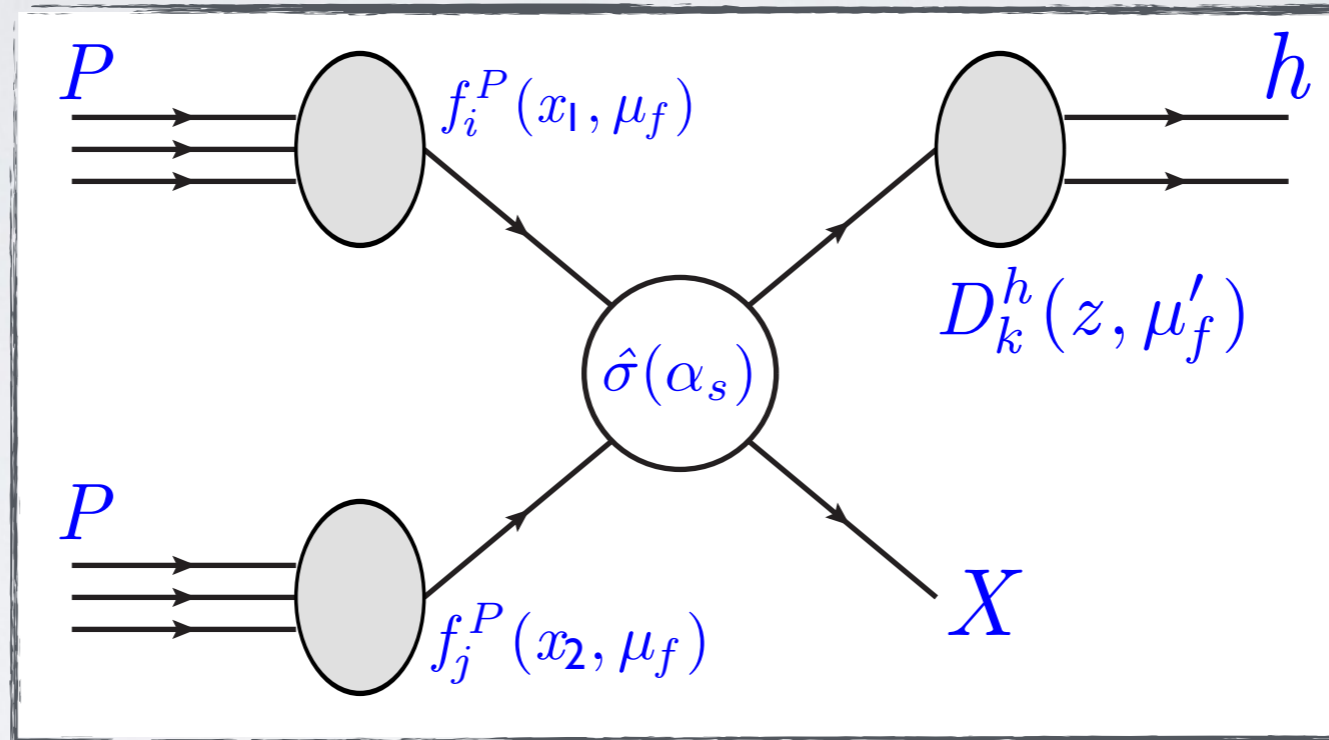
Altarelli et al. '79, Furmanski, Petronzio '82, de Florian, Stratmann, Vogelsang '98

- Charge and flavour separation is achieved by including SIDIS.
- However, gluon FF is not well constrained by SIA and SIDIS data.



FFs in data: Hadron collisions

- The general picture is:



- Therefore, transverse momentum distribution is given by:

$$\frac{d\sigma(pp \rightarrow hX)}{dp_T d\eta} = \sum_{i,j,k} \int dx_1 dx_2 dz \left[f_i^P(x_1, \mu_f) f_j^P(x_2, \mu_f) D_k^h(z, \mu'_f) \frac{d\hat{\sigma}(ij \rightarrow kX')}{dp_T d\eta} \right]$$

- It also allows charge and flavour separation.
- It contains large contributions from gluons.

DSS vs the new fit

- Number of parameters: 23 parameters > 28 parameters.
- HERMES data are replaced and added deuteron target data sets.
- Different treatment for the normalization of the experiments.
- PDFs: MSTW2008.
- Relaxing some of the FFs assumptions.

$$D_i^{\pi^+}(z, Q_0) = \frac{N_i z^{\alpha_i} (1-z)^{\beta_i} [1 + \gamma_i (1-z)^{\delta_i}]}{B[2 + \alpha_i, \beta_i + 1] + \gamma_i B[2 + \alpha_i, \beta_i + \delta_i + 1]}$$

$$D_{d+\bar{d}}^{\pi^+} = N_{d+\bar{d}} D_{u+\bar{u}}^{\pi^+} \quad D_{\bar{u}}^{\pi^+} = D_d^{\pi^+}$$

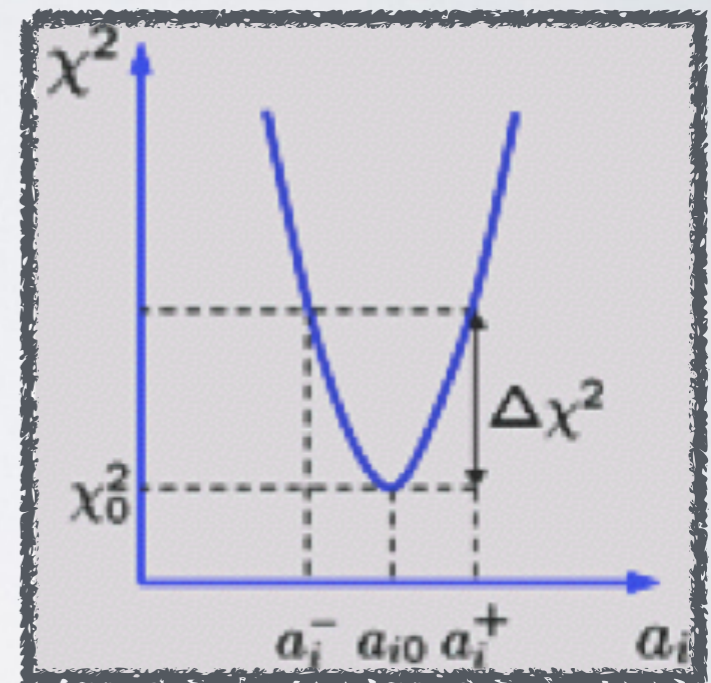
$$D_s^{\pi^+} = D_{\bar{s}}^{\pi^+} = N_s z^{\alpha_s} D_{\bar{u}}^{\pi^+} \quad \gamma_{c,b} \neq 0$$

Uncertainties

Goal: Provide Hessian sets to propagate FFs uncertainties.

HESSIAN METHOD

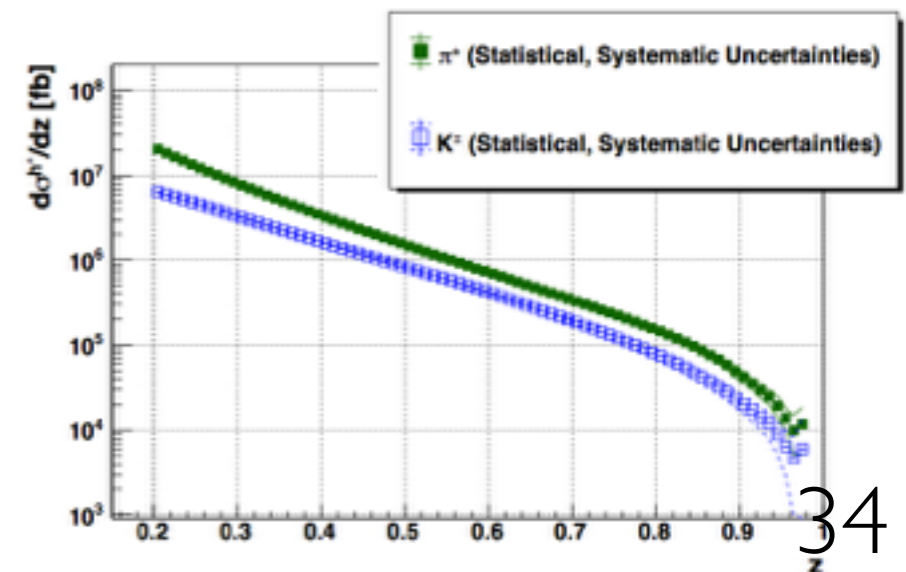
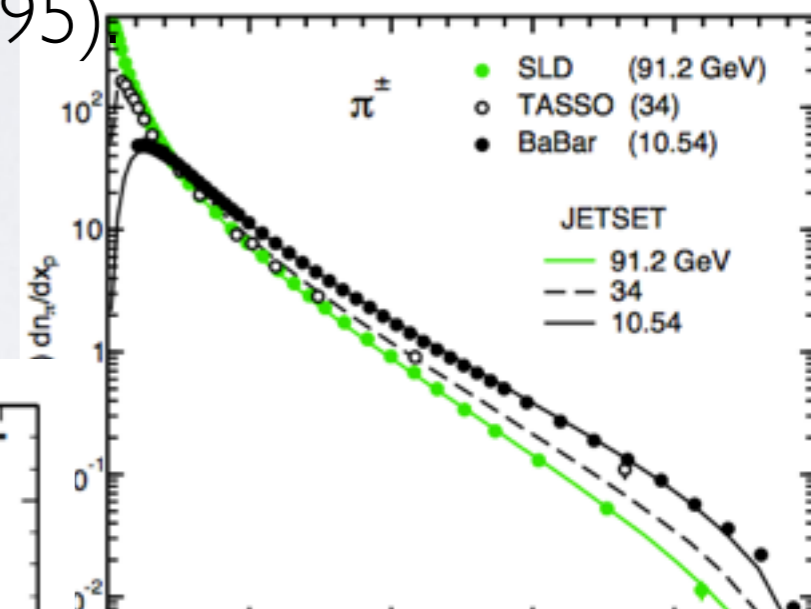
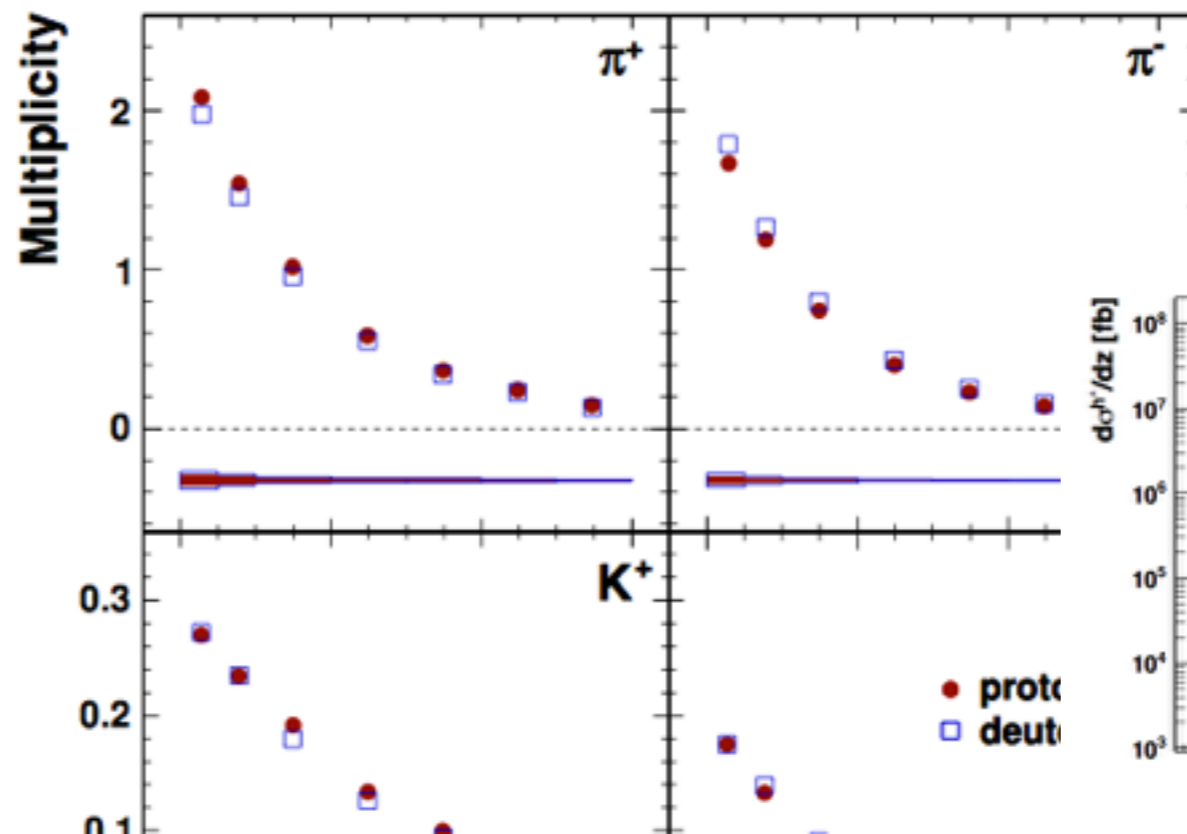
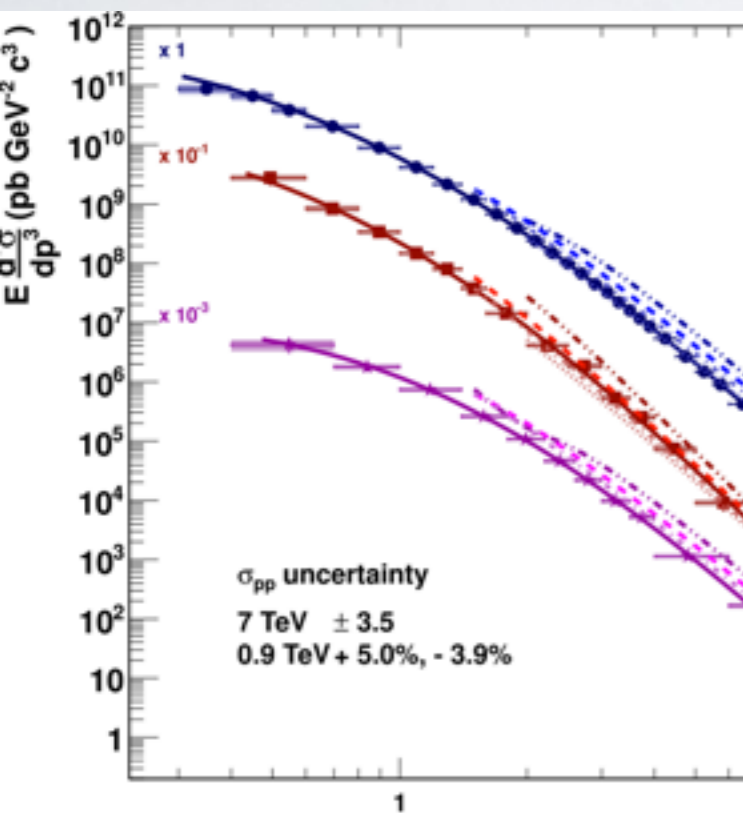
- Idea: Explore the vicinity of the best fit in quadratic approximation.
- Caveat: Quadratic approximation is not exactly what is used for the global fits, i.e. PDFs too.
- However, it is a good test of the convergence of the fitting procedure.



$$D_i^{\pi^+}(z, Q_0) = \frac{N_i z^{\alpha_i} (1-z)^{\beta_i} [1 + \gamma_i (1-z)^{\delta_i}]}{B[2 + \alpha_i, \beta_i + 1] + \gamma_i B[2 + \alpha_i, \beta_i + \delta_i + 1]}$$

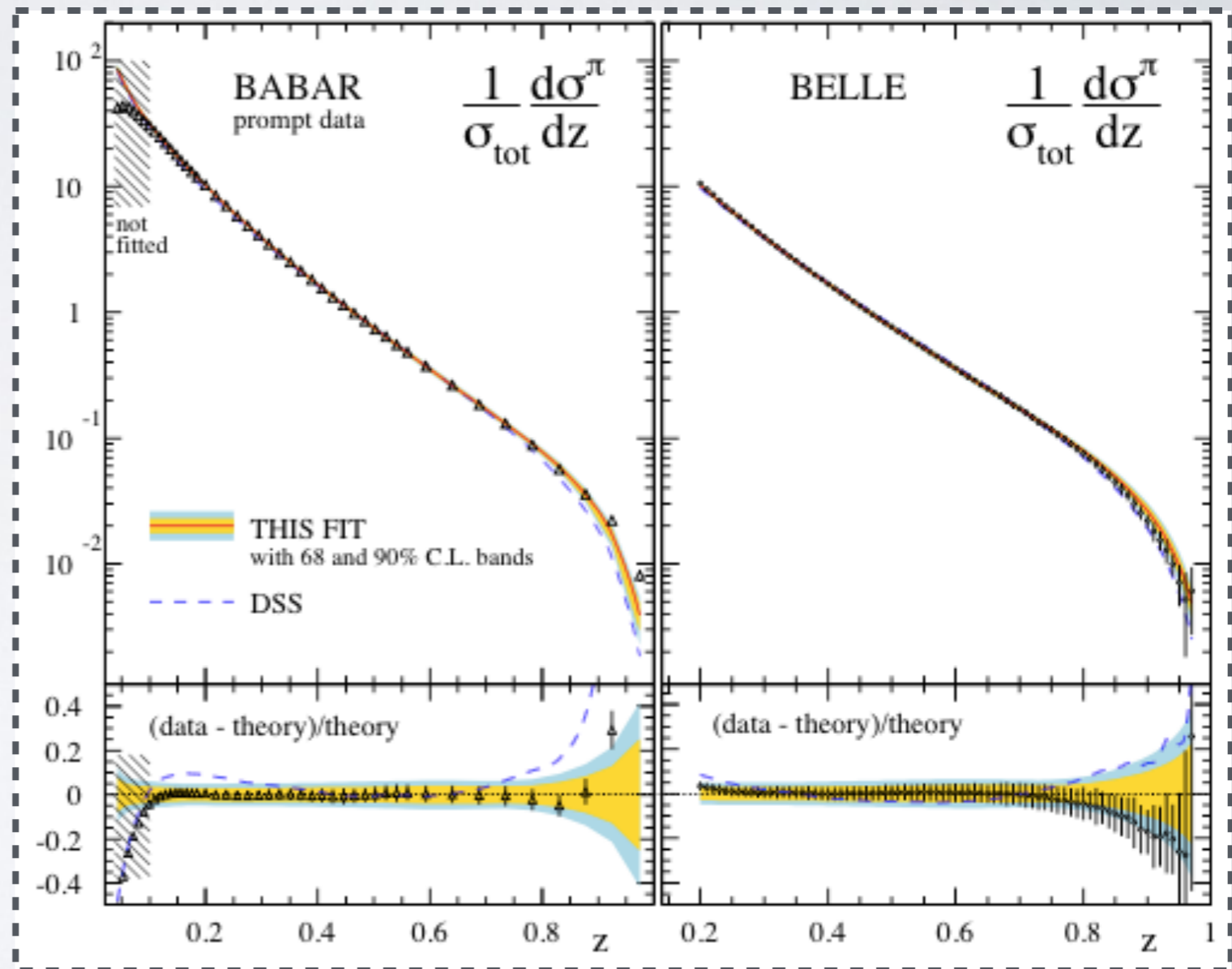
— *New data to fit* —

- New data from PHENIX and STAR (Phys.Rev.C81(2010)064904; PRL 108(2012)072302;...).
- Data from the LHC (Phys.Lett.B717(2012)162;1307.1093;...).
- e+e- data from BELLE(1301.6183) and BaBar (1306.2895)
- SIDIS multiplicities from COMPASS (1307.3407).
- Final SIDIS multiplicities from HERMES (1212.5407).



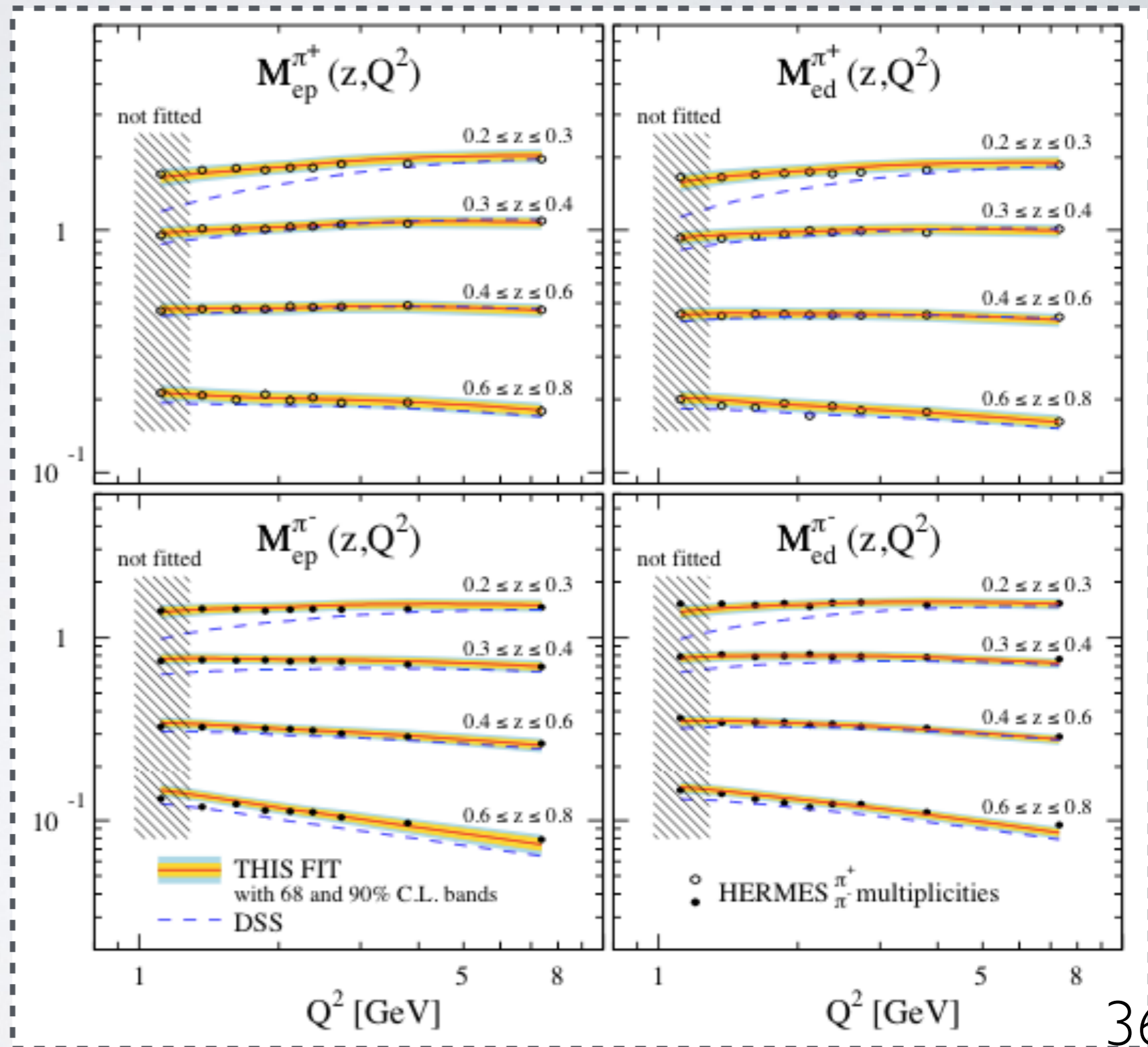
BELLE & BaBar

- BELLE and BaBar results can be fitted extremely well within the 68 and 90 % C.L.
- There is a drop on the large z regime for BELLE but it is consistent with the uncertainties.
- Large logarithmic corrections are expected at large values of z .
- Sensitive to a partial flavour separation



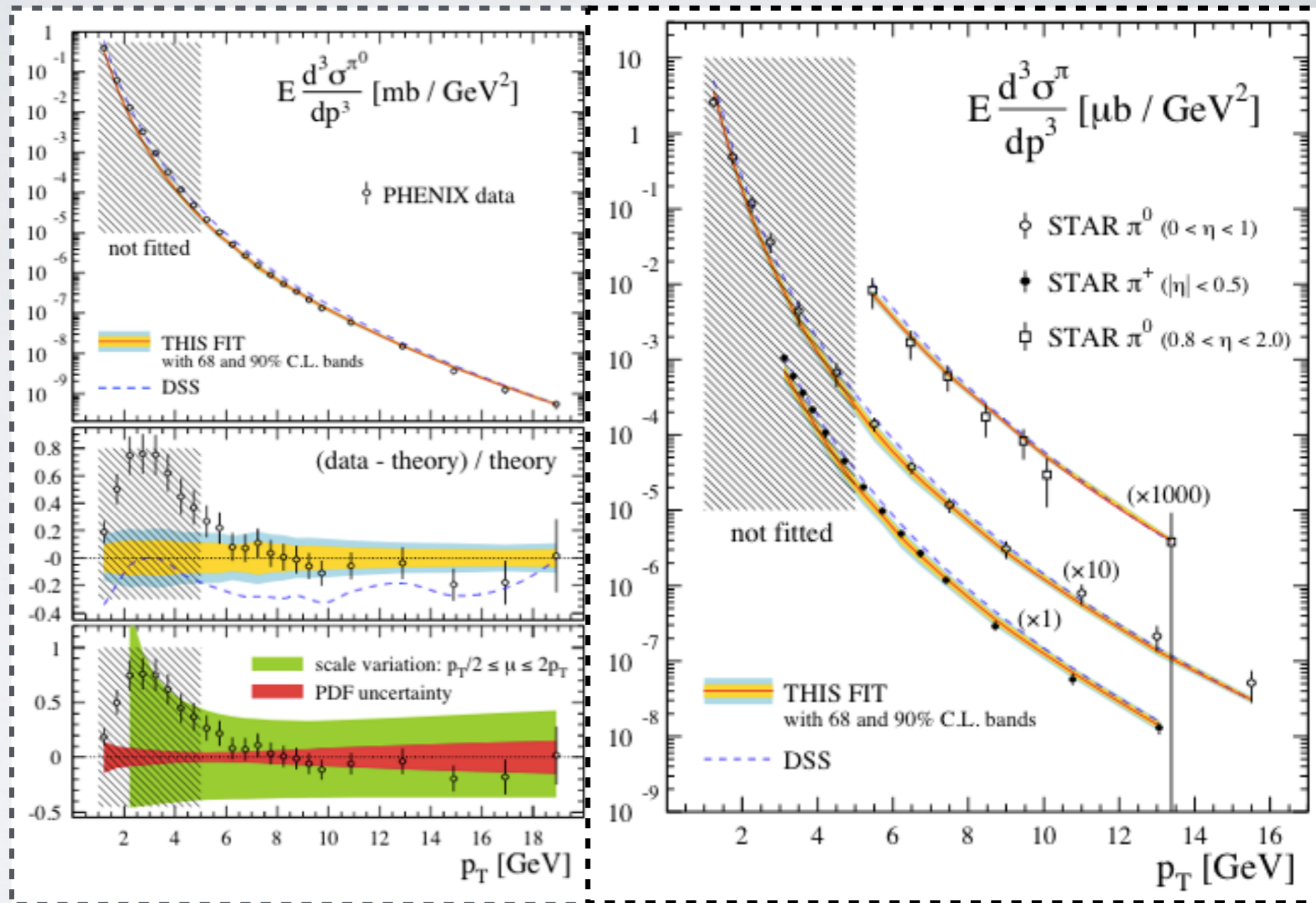
HERMES

- DSS cannot fit the new HERMES data for the smallest bin of z .
- In this new analysis, HERMES data have no problems to be fitted within the 68 and 90% C.L. for all bins of z .



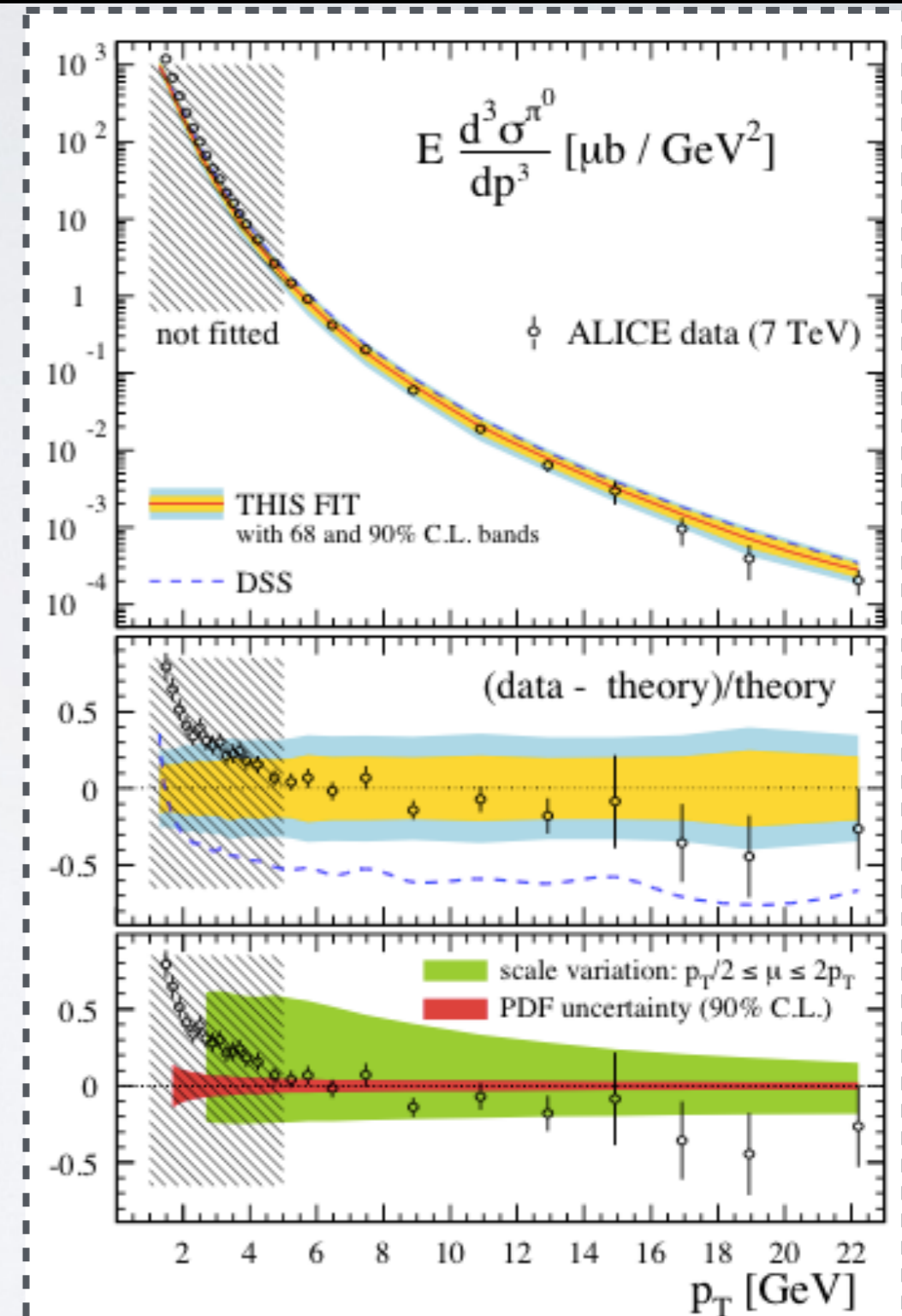
PHENIX & STAR

PDF uncertainties where computed with 90%CL MSTW and they are less significant than the scale ambiguities.



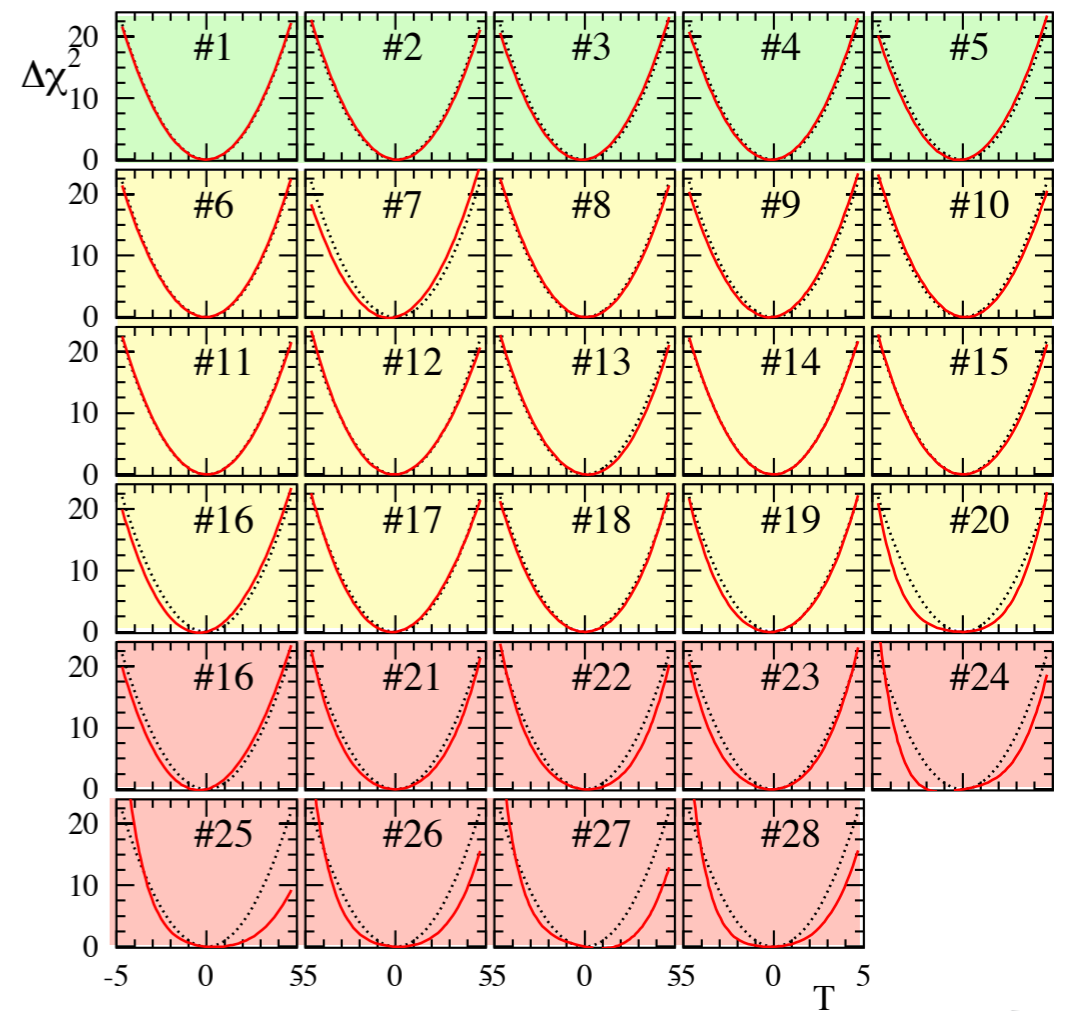
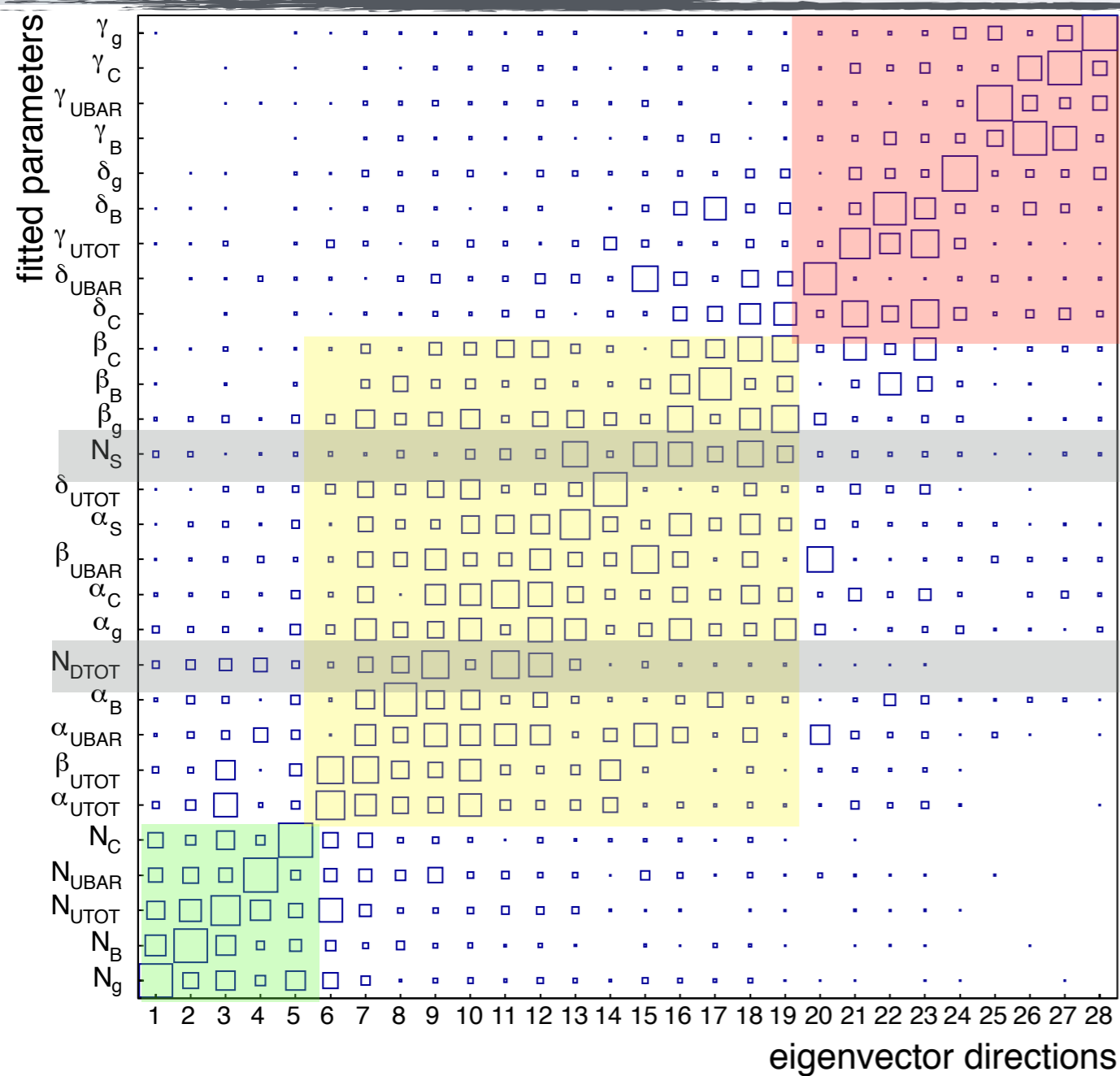
ALICE

- In the range of small p_T , RHIC and LHC data showed a tension during the fitting.
- By introducing the cut on the p_T , we achieved a reasonable agreement between both data sets.
- Nevertheless, we lost some data sets such as ALICE 900GeV which only stands with one point.
- Contribution of uncertainties due to PDF are again not relevant enough; the main contribution is coming from the scale variation.



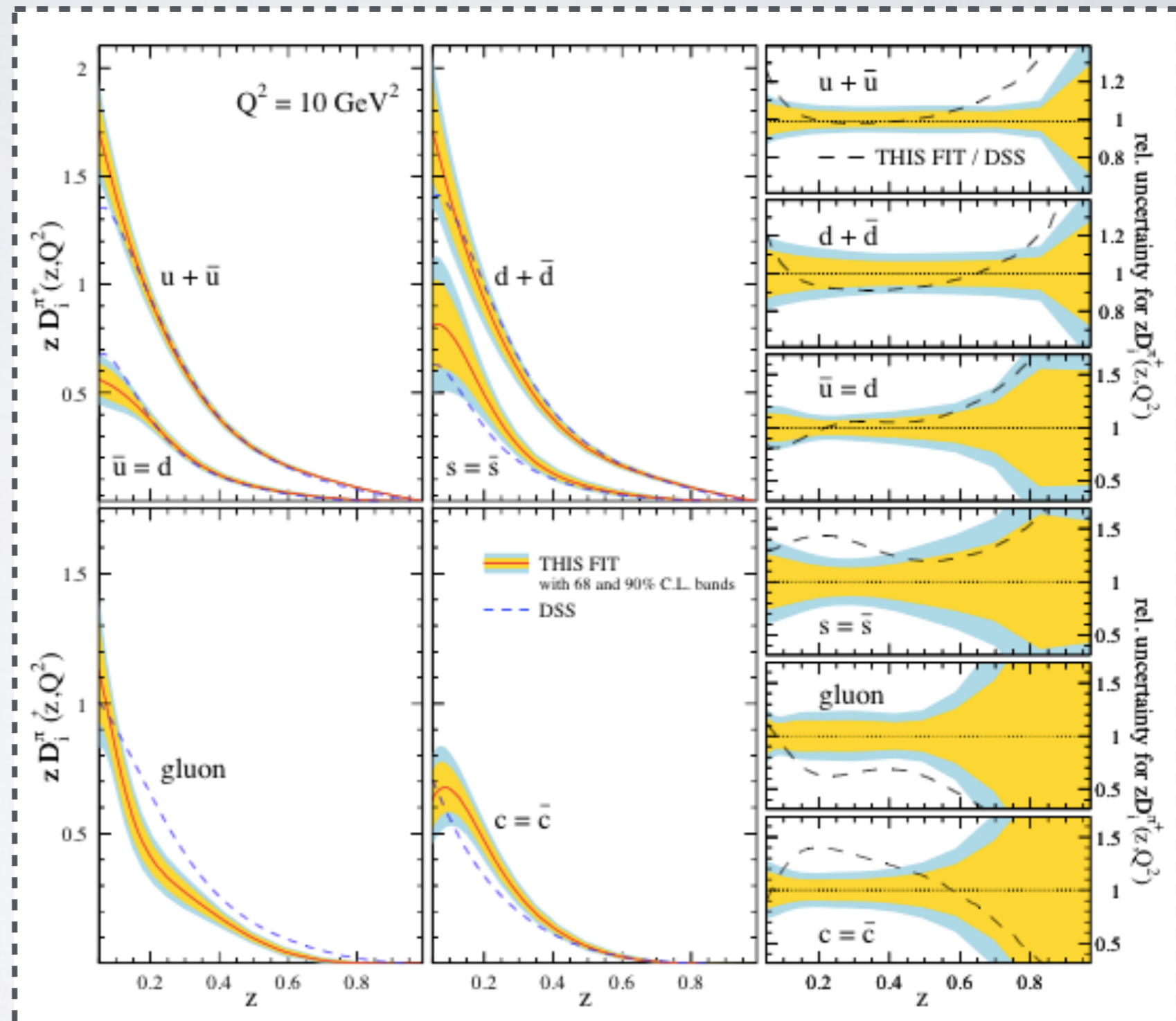
Hessian method & convergence

$$D_i^{\pi^+}(z, Q_0^2) = N_i z^{\alpha_i} [(1-z)^{\beta_i} + \gamma_i (1-z)^{\delta_i}]$$



parton-to-pion FFs

- Deviations from DSS is found on the gluon and charm FF.
- c-FF has a more flexible parametrisation (5 instead of 3 parameters).
- g-FF uncertainties is about 20% at 90%CL up to $z > 0.5$ and they increase towards larger values ($Q = 10 \text{ GeV}$).



How good is the fit ?

	DSS	NOW
Global	843/392(2.15)	1154.6/973(1.19)
LEP-SLAC	500.1/260(1.92)	412.6/260(1.58)
BELLE & BABAR	—	90.4/123(0.73)
HERMES	188.2/64(2.94)	175/128(1.36)
COMPASS	—	403.2/398(1.01)
RHIC	160.8/68(2.36)	45.7/53(0.86)
LHC	—	27.7/11(2.51)

— *Conclusions* —

- New methods for computing higher order corrections are needed for upcoming LHC observables.
- Mapping of momenta between real and virtual corrections permits to cancel soft and final-state collinear singularities.
- Fully local cancellation of IR and UV divergences through the LTD.
- LTD allows to build an algorithm for computing 4-dimensional representations of NLO cross sections.
- Extension of the LTD at NNLO and multi-leg processes is on the way.

— *Conclusions* —

- The numerical results shown that the breaking of the charge asymmetry parameter is very close to one.
- Tension between RHIC & LHC data have been avoided when a lower cut is introduced in the proton-proton collisions.
- The new data do not favor any symmetry violation.
- Uncertainties have been estimated using the standard iterative Hessian method.
- The analysis implemented strongly supports factorization and universality for the parton-to-pion FFs.

THANKS...
